

## Corrections to chiral dynamics of heavy hadrons: SU(3) symmetry breaking

Hai-Yang Cheng,<sup>1,4</sup> Chi-Yee Cheung,<sup>1</sup> Guey-Lin Lin,<sup>1</sup> Y. C. Lin,<sup>2</sup> Tung-Mow Yan,<sup>3</sup> and Hoi-Lai Yu<sup>1</sup>

<sup>1</sup>*Institute of Physics, Academia Sinica, Taipei, Taiwan 11529, Republic of China*

<sup>2</sup>*Physics Department, National Central University, Chung-li, Taiwan 32054, Republic of China*

<sup>3</sup>*Floyd R. Newman Laboratory of Nuclear Studies, Cornell University, Ithaca, New York 14853*

<sup>4</sup>*Institute for Theoretical Physics, State University of New York, Stony Brook, New York 11794*

(Received 23 December 1993)

In previous publications we have analyzed the strong and electromagnetic decays of heavy mesons and heavy baryons in a formalism which incorporates heavy-quark and chiral symmetries. There are two possible symmetry-breaking effects on the chiral dynamics of heavy hadrons: the finite-mass effects from light quarks and the  $1/m_Q$  corrections from heavy quarks. In the present paper, chiral-symmetry-breaking effects are studied and applications to various strong and radiative decays of heavy hadrons are illustrated. SU(3) violations induced by chiral loops in the radiative decays of charmed mesons and charmed baryons are compared with those predicted by the constituent quark model. In particular, available data for  $D^*$  decays favor values of the parameters in chiral perturbation theory which give predictions for  $D^*$  decays close to the quark model results except for the  $D_s^{*+}$ . Implications are discussed.

PACS number(s): 11.30.Rd, 12.39.Hg, 13.25.Ft, 13.40.Hq

### I. INTRODUCTION

The dominant decay modes of many heavy hadrons, which contain a heavy quark, are strong decays with one soft pion emission and/or electromagnetic decays. This is a consequence of the heavy quark symmetry [1,2] of QCD: Mass differences among the different spin multiplets of the ground-state heavy mesons and heavy baryons are generally small. An ideal framework for studying the low-energy dynamics of heavy hadrons is provided by the formalism in which the heavy quark symmetry and the chiral symmetry are synthesized [3–10]. However, symmetry considerations alone in general do not give any quantitative predictions unless further assumptions are made. Fortunately, all the unknown parameters in the Lagrangian depend only on the light quarks and are calculable from the nonrelativistic quark model. In Refs. [3,9,10] (for later convenience, Refs. [3] and [10] will be denoted as papers I and II, respectively), we have explored in detail the predictions of this theoretical formalism on strong decays, radiative decays, and heavy-flavor-conserving nonleptonic decays.

In this and a preceding paper, we would like to examine various symmetry-breaking corrections to the strong and radiative decays of heavy mesons and baryons. There are two different kinds of symmetry-breaking effects on the chiral dynamics of heavy hadrons: the finite-mass effects from the light quarks and the  $1/m_Q$  corrections from the heavy quarks. In paper II we have already incorporated one of the  $1/m_Q$  effects, namely, the magnetic moment of the heavy quark, into the formalism for describing the electromagnetic ( $M1$ ) decay of heavy hadrons. This is because the charmed quark is not particularly heavy, and hence the contribution due to its magnetic moment cannot be safely neglected.

There are two strong motivations, among others, for promoting a systematic study of both the  $1/m_Q$  correc-

tions and the effects of chiral symmetry breaking. First, we have calculated in paper II the decay rates of  $D^* \rightarrow D\gamma$ . When combined with our prediction for the strong decays  $D^* \rightarrow D\pi$  given in paper I, we are able to predict the branching ratios for the  $D^*$  decays. Agreement is excellent between theory and the most recent experiment of CLEO II [11]. Nevertheless, our predicted total width for  $D^{*+}$  is<sup>1</sup>  $\Gamma_{\text{tot}}(D^{*+}) = 150$  keV, which is to be compared with the upper limit  $\Gamma_{\text{tot}}(D^{*+}) < 131$  keV published by the ACCMOR Collaboration [12]. We thus urge the experimentalists to perform more precision measurements of the  $D^*$  total width. Therefore it becomes urgent to analyze the symmetry-breaking effects on the strong decays  $D^* \rightarrow D\pi$  and the radiative decays  $D^* \rightarrow D\gamma$ . This is particularly so should the aforementioned upper limit for  $\Gamma_{\text{tot}}(D^{*+})$  be confirmed by future experiments. Second, to the lowest-order chiral Lagrangian, there exist several SU(3) relations among the radiative decay amplitudes of heavy mesons and heavy baryons, for example,  $A(D^{*+} \rightarrow D^+\gamma) = A(D_s^{*+} \rightarrow D_s^+\gamma)$ . Therefore observation of different rates for the decays  $D^{*+} \rightarrow D^+\gamma$  and  $D_s^{*+} \rightarrow D_s^+\gamma$  (after taking into account mass differences between  $D^{+(*)}$  and  $D_s^{+(*)}$ ) will clearly signal the SU(3) flavor symmetry breaking due to the light current quark masses. In paper II, the magnetic moments of heavy hadrons are related to the magnetic moments of the constituent quarks in the nonrelativistic quark model. In this approach, SU(3) violations in radiative ( $M1$ ) decays arise from the constituent quark mass differences. In the present work, we shall follow the orthodox approach of chiral perturbation theory to treat

<sup>1</sup>The difference between this number (see Table I) and the result 141 keV obtained in Ref. [10] is due to the fact that here we have used a more accurate pion momentum.

SU(3)-breaking effects: The coupling constants in the Lagrangian are treated to be invariant, and all SU(3) violations of interest are induced by chiral loops. A comparison of these two different approaches of SU(3) breaking is given in the end. Existing data for the  $D^*$  decays, though limited, favor a set of parameters such that chiral perturbation theory and the quark model give similar results for the  $D^*$  decays, but not for  $D_s^{*+} \rightarrow D_s^+ \gamma$ . In addition, even if the upper limit for the total width of  $D^{*+}$  [12] is to be taken seriously, it does not pose a difficulty in the chiral perturbation theory approach. For the heavy baryons, lack of any data prevents us from making a meaningful search for an optimum choice of parameters in chiral perturbation theory.

Since both symmetry-breaking effects require a careful and thorough study, we focus on the SU(3) symmetry breaking in this paper. A detailed investigation of  $1/m_Q$  corrections has been carried out in a preceding paper [13]. Schematically, the general effective chiral Lagrangian in chiral perturbation theory (ChPT) involving heavy hadrons has the chiral expansion

$$\mathcal{L} = \mathcal{L}_1 + \mathcal{L}_2 + \mathcal{L}_3 + \cdots, \quad (1.1)$$

where the subscript denotes the sum of the number of derivatives acting on the Goldstone fields and the velocity-dependent heavy hadron fields, and the power of the Goldstone-boson mass squared in the Lagrangian.<sup>2</sup> (Recall that the lowest-order chiral-symmetry-breaking terms are linear in light quark masses and hence quadratic in Goldstone-boson masses.) The higher-order chiral Lagrangians are suppressed by powers of  $p/\Lambda_\chi$  or  $m^2/\Lambda_\chi^2$ , where  $p(m)$  is the momentum (mass) of the Goldstone bosons and  $\Lambda_\chi$  is a chiral-symmetry-breaking scale  $\sim 1$  GeV [14]. Therefore perturbation theory makes sense if  $p$  and  $m$  are not too large compared to  $\Lambda_\chi$ . Chiral corrections of interest usually receive two contributions: one from the chiral loops generated by  $\mathcal{L}_1$  and the other from the higher-order tree Lagrangian term  $\mathcal{L}_2$ . Loop contributions can be either finite or divergent. The divergent part typically has the form (see Appendix A)

$$\frac{2}{\epsilon} - \gamma_E + \ln 4\pi + 1 + \frac{1}{2} \ln \frac{\Lambda^2}{m^2} \quad (1.2)$$

in the dimensional regularization scheme, where  $\epsilon = 4 - n$  and  $\Lambda$  is an arbitrary renormalization scale. In ChPT, all divergences from chiral loops induced by<sup>3</sup>  $\mathcal{L}_1$  will be absorbed into the counterterms which have the same structure as that of  $\mathcal{L}_2$  [15]. Denoting the bare parameters of  $\mathcal{L}_2$  by  $f_i$ , the renormalized parameters  $f_i^r$  are then given

by [16]

$$f_i^r(\Lambda) = f_i + \frac{\gamma_i}{32\pi^2} \left[ \frac{2}{\epsilon} - \gamma_E + \ln 4\pi + 1 \right] \Lambda^\epsilon, \quad (1.3)$$

with  $\gamma_i$  being calculable coefficients. We see that although the lowest-order chiral Lagrangian  $\mathcal{L}_1$  is scale independent, renormalized higher-order effective Lagrangians do depend on the choice of  $\Lambda$ , reflecting the non-renormalizability nature of ChPT. Of course, physical amplitudes should be independent of the renormalization scale; that is, the  $\Lambda$  dependence from the chiral loop is exactly compensated by the  $\Lambda$  dependence of local counterterms in  $\mathcal{L}_2$ . As the renormalized parameters  $f_i^r$  are unknown and must be determined from experiment, we will thus concentrate in the present paper on the chiral corrections due to meson loops. Furthermore, we will choose  $\Lambda \sim \Lambda_\chi$  to get numerical estimates of chiral-loop effects.

Chiral-loop corrections to some heavy meson processes have been discussed by other authors [8,17–20]. In the heavy baryon sector, the only chiral-loop effects studied so far are those in Ref. [17] on the semileptonic decays. In this paper we attempt to make a systematic and complete investigation of chiral-loop corrections to the strong and electromagnetic decays of heavy hadrons. They arise from the chiral-symmetry-breaking terms in (1.1) and hence vanish in the chiral limit. The leading chiral-loop effects we found are nonanalytic in the forms of  $m/\Lambda_\chi$  and  $(m^2/\Lambda_\chi^2) \ln(\Lambda^2/m^2)$  (or  $m_q^{1/2}$  and  $m_q \ln m_q$ , with  $m_q$  being the light quark mass). Furthermore, they amount to finite-light-quark-mass corrections to the coupling constant, say  $g$ , in  $\mathcal{L}_1$ . Schematically,

$$g_{\text{eff}} = g \left[ 1 + O \left[ \frac{m}{\Lambda_\chi} \right] + O \left[ \frac{m^2}{\Lambda_\chi^2} \ln \frac{\Lambda^2}{m^2} \right] + O(m^2) \bar{g}^r(\Lambda) \right], \quad (1.4)$$

where  $\bar{g}^r(\Lambda)$  is the relevant renormalized coupling constant in  $\mathcal{L}_2$ ; that is, the chiral-loop and  $\mathcal{L}_2$  contributions have the same structure as the  $g$  term in  $\mathcal{L}_1$  except that they vanish in the chiral limit. This point will be elaborated on again in Sec. II. In this work we shall only keep the nonanalytic loop effects.

The present paper is organized as follows. In Sec. II we calculate chiral corrections to the strong decay  $P^* \rightarrow P\pi$  and the radiative decay  $P^* \rightarrow P\gamma$ , where  $P^*$  and  $P$  refer to  $1^-$  and  $0^-$  ground-state vector and pseudoscalar mesons, respectively. As noted earlier, the  $1/m_Q$  effect due to the magnetic moment of the heavy quark is included. Similar chiral-loop calculations are presented for heavy baryons in Sec. III, except there we adopt velocity-dependent “superfields” which combine spin- $\frac{1}{2}$  and spin- $\frac{3}{2}$  sextet baryon fields together [6,17]. Computation becomes much simplified in this compact notation. A by-product of our investigation of Secs. II and III is the confirmation at the one-loop level of an exact QCD result (see [13], for example) that the coupling constants

<sup>2</sup>For pure Goldstone-boson fields, the chiral expansion of chiral Lagrangians has the familiar form  $\mathcal{L} = \mathcal{L}_2 + \mathcal{L}_4 + \mathcal{L}_6 + \cdots$ . In this case, higher-order chiral terms are suppressed by powers of  $p^2/\Lambda_\chi^2$  or  $m^2/\Lambda_\chi^2$ .

<sup>3</sup>The quadratic divergence, if it exists, usually amounts to renormalizing  $\mathcal{L}_1$ . In the dimensional regularization scheme, we only focus on those logarithmic divergences.

due to heavy quarks in the  $M1$  transitions of both heavy mesons and baryons are not modified by the light quark dynamics. In Sec. IV we consider applications of our results to the strong and electromagnetic decays of charmed mesons and charmed baryons. SU(3) violation induced by chiral loops for the radiative decays is compared with that predicted by the nonrelativistic quark model. Section V contains conclusions and outlook. Two appendixes are devoted to some technical details.

## II. SU(3)-SYMMETRY-BREAKING CORRECTIONS TO THE CHIRAL DYNAMICS OF HEAVY MESONS

In this section we shall study the chiral-symmetry-breaking effects on the strong and electromagnetic decays of heavy mesons. To begin with, we recall the lowest-order gauge-invariant chiral Lagrangians (I.2.20) and (II.2.19) for heavy mesons,

$$\begin{aligned} \mathcal{L}_{v,PP^*}^{(1)} = & -2iM_{P^*}P(v) \cdot DP^\dagger(v) + 2iM_{P^*}P^{*\mu}(v)v \cdot DP_\mu^{*\dagger}(v) + \Delta M^2 P(v)P^\dagger(v) \\ & + f\sqrt{M_P M_{P^*}} \epsilon_{\mu\nu\alpha\beta} [P(v)\mathcal{A}^\mu P_\mu^{*\dagger}(v) + P_\mu^*(v)\mathcal{A}^\mu P^\dagger(v)] + 2igM_{P^*} \epsilon_{\mu\nu\lambda\kappa} P^{*\mu}(v)v^\nu \mathcal{A}^\lambda P^{*\kappa\dagger}(v) \end{aligned} \quad (2.1)$$

and

$$\begin{aligned} \mathcal{L}_{v,PP^*}^{(2)} = & \sqrt{M_P M_{P^*}} \epsilon_{\mu\nu\alpha\beta} v^\alpha P^{*\beta}(v) [\frac{1}{2}d(\xi^\dagger Q\xi + \xi Q\xi^\dagger) + d'Q'] F^{\mu\nu} P^\dagger(v) + \text{H. c.} \\ & + id''M_{P^*} F_{\mu\nu} P^{*\nu}(v) [\gamma Q' - \frac{1}{2}(\xi^\dagger Q\xi + \xi Q\xi^\dagger)] P^{*\mu\dagger}(v), \end{aligned} \quad (2.2)$$

with  $\Delta M^2 = M_{P^*}^2 - M_P^2$ ,

$$\begin{aligned} P_{\mu\nu}^{*\dagger} &= D_\mu P_\nu^{*\dagger} - D_\nu P_\mu^{*\dagger}, \\ P_{\mu\nu}^* &= D_\mu P_\nu^* - D_\nu P_\mu^*, \end{aligned} \quad (2.3)$$

where  $P$  and  $P^*$  denote the ground-state  $0^-$  and  $1^-$  heavy mesons, respectively, which contain a heavy quark  $Q$  and a light antiquark  $\bar{q}$ ,  $\mathcal{V}_\mu$  and  $\mathcal{A}_\mu$  are the respective chiral vector and axial fields (see paper II for more detail),  $Q = \text{diag}(\frac{2}{3}, -\frac{1}{3}, -\frac{1}{3})$  is the charge matrix for the light  $u$ ,  $d$ , and  $s$  quarks,  $Q'$  (or  $e_Q$ ) is the charge of the heavy quark,  $\xi = \exp(iM/\sqrt{2}f_0)$  with the unrenormalized decay constant  $f_0$  to be determined later, and  $M$  is the meson matrix of Goldstone-boson fields,

$$M \equiv \sum_a \frac{\lambda^a \pi^a}{\sqrt{2}} = \begin{pmatrix} \frac{\pi^0}{\sqrt{2}} + \frac{\eta}{\sqrt{6}} & \pi^+ & K^+ \\ \pi^- & -\frac{\pi^0}{\sqrt{2}} + \frac{\eta}{\sqrt{6}} & K^0 \\ K^- & \bar{K}^0 & -(\frac{2}{3})^{1/2}\eta \end{pmatrix}, \quad (2.4)$$

where the  $\lambda$ 's are the Gell-Mann matrices normalized by  $\text{tr}(\lambda^a \lambda^b) = 2\delta^{ab}$ . It should be stressed that the Lagrangians (2.1) and (2.2) are expressed in terms of velocity-dependent heavy fields.

The covariant derivative  $D_\mu$  in Eqs. (2.1)–(2.3) is defined by

$$\begin{aligned} D_\mu P &= \partial_\mu P + \mathcal{V}_\mu^* P + ie A_\mu (Q' P - P Q), \\ D_\mu P_\nu^\dagger &= \partial_\mu P_\nu^\dagger + \mathcal{V}_\mu P_\nu^\dagger - ie A_\mu (P_\nu^\dagger Q' - Q P_\nu^\dagger), \end{aligned} \quad (2.5)$$

with  $\mathcal{V}_\mu = \frac{1}{2}[\xi^\dagger D_\mu \xi + \xi (D_\mu \xi)^\dagger]$ . The covariant derivative in  $\mathcal{V}_\mu$  contains the photon field  $A_\mu$  to incorporate the

electromagnetic interactions of the Goldstone bosons; explicitly,

$$D_\mu \xi = \partial_\mu \xi + ie A_\mu [Q, \xi]. \quad (2.6)$$

In Eq. (2.2),  $v$  is the velocity of heavy mesons and the two coupling constants  $dQ$  and  $d''Q$  can be related to the magnetic moments of light constituent quarks in the quark model. The universal coupling constants  $d$  and  $d''$  are independent of the heavy quark masses and species. We have also included the  $d'Q'$  and  $\gamma Q'$  terms to account for the corrections due to the heavy quark masses when  $m_Q \neq \infty$ . The coupling constants  $f$  and  $g$  in (2.1) and  $d$  and  $d''$  in (2.2) are related by heavy quark symmetry as [3,10]

$$f = 2g, \quad d'' = -2d. \quad (2.7)$$

Moreover, the couplings  $d'$  and  $d''\gamma$  are fixed by heavy quark symmetry to be [10]

$$d' = -\frac{e}{2m_Q}, \quad d''\gamma = \frac{e}{m_Q}. \quad (2.8)$$

We shall see that from the lowest-order Lagrangians given by (2.1) and (2.2) there is an SU(3) prediction:  $A(D^{*+} \rightarrow D^+ \gamma) = A(D_s^{*+} \rightarrow D_s^+ \gamma)$ . Therefore observation of different rates for the radiative decays of  $D^{*+}$  and  $D_s^{*+}$  (after taking into account the mass difference of  $D^{+(\ast)}$  and  $D_s^{+(\ast)}$ ) will evidently signal the SU(3)-breaking effects induced by the light quark masses. In chiral perturbation theory, the masses of light quarks are treated as a small perturbation and SU(3) violation in radiative decays is induced by chiral loops. In paper II, the unknown coupling constants  $d$  and  $d''$  in (2.2) are derived from the nonrelativistic quark model and they are related to the masses of the constituent  $u$ ,  $d$ , and  $s$  quarks. As a

consequence, SU(3) violation is already incorporated into the “effective” couplings  $d$  and  $d''$  in paper II. In this paper we shall adopt the orthodox approach of chiral perturbation theory for treating SU(3)-breaking effects. As will be shown, leading chiral corrections have nonanalyt-

ic dependence on  $m_q$  of the form  $m_q^{1/2}$  or  $m_q \ln m_q$ . In Sec. IV the above two different approaches for SU(3) violation in radiative decays of heavy hadrons will be compared.

The chiral-symmetry-breaking terms are given by

$$\begin{aligned} \mathcal{L}_{\text{CSB}} = & \frac{f_0^2}{2} B_0 \text{tr}(\mathcal{M}^\dagger \Sigma + \Sigma^\dagger \mathcal{M}) + \alpha_1 M_P P(v) (\xi \mathcal{M}^\dagger \xi + \xi^\dagger \mathcal{M} \xi^\dagger) P^\dagger(v) + \alpha_2 M_{P^*} P^*(v) (\xi \mathcal{M}^\dagger \xi + \xi^\dagger \mathcal{M} \xi^\dagger) P^{*\dagger}(v) \\ & + \alpha_3 M_P P(v) P^\dagger(v) \text{tr}(\mathcal{M}^\dagger \Sigma + \Sigma^\dagger \mathcal{M}) + \alpha_4 M_{P^*} P^*(v) P^{*\dagger}(v) \text{tr}(\mathcal{M}^\dagger \Sigma + \Sigma^\dagger \mathcal{M}), \end{aligned} \quad (2.9)$$

where  $\Sigma = \xi^2$ ,  $B_0 = -4 \langle \bar{q}q \rangle / f_0^2$  characterizes the spontaneous breaking of chiral symmetry, and  $\mathcal{M}$  is a light quark mass matrix:

$$\mathcal{M} = \begin{pmatrix} m_u & 0 & 0 \\ 0 & m_d & 0 \\ 0 & 0 & m_s \end{pmatrix}. \quad (2.10)$$

The unknown dimensionless parameters  $\alpha_i$  are expected to be of order unity (see Sec. IV for more discussion). Each symmetry-breaking term in (2.9) transforms either as  $(\bar{3}, 3)$  or  $(3, \bar{3})$  under  $\text{SU}(3)_L \times \text{SU}(3)_R$ . As the symmetry-breaking effect is purely induced by the light quark masses,  $\mathcal{L}_{\text{CSB}}$  should be independent of the heavy quark mass and spin. By comparing (2.9) with (2.1), this immediately gives  $\alpha_1 = -\alpha_2$  and  $\alpha_3 = -\alpha_4$ . As one can see from (2.9),  $\mathcal{L}_{\text{CSB}}$  does not break the heavy quark symmetry (HQS) relations given by Eq. (2.7). In fact, chiral symmetry breaking should preserve HQS as light meson interactions have nothing to do with the heavy quarks.

We shall first calculate the chiral-loop contributions to the strong decay  $P_i^* \rightarrow P_j + \pi^a$  as depicted in Fig. 1, where  $P_i$  denotes  $(Q\bar{u}, Q\bar{d}, Q\bar{s})$  and likewise for  $P_i^*$ . The tree amplitude can be read out from (2.1) to be

$$A [P_i^* \rightarrow P_j \pi^a(q)]_{\text{tree}} = \frac{g}{f_0} \sqrt{M_P M_{P^*}} (\lambda^a)_{ij} (\epsilon^* \cdot q). \quad (2.11)$$

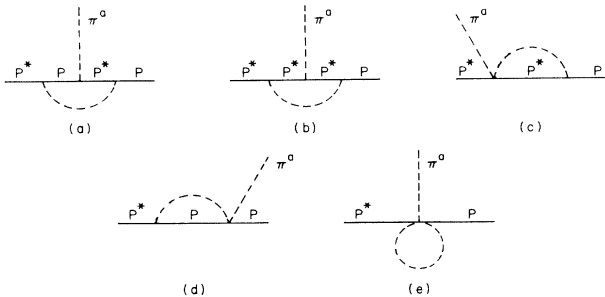


FIG. 1. Chiral-loop diagrams contributing to the strong decay  $P^* \rightarrow P \pi^a$ . For simplicity, the wave-function renormalization and mass counterterms are not shown in Figs. 1–8, but the necessary mass renormalization is to be understood.

As discussed in the Introduction, the loop-induced logarithmic divergence is absorbed into the chiral-symmetry-breaking counterterms

$$\begin{aligned} a P(v) (\xi \mathcal{M}^\dagger \xi + \xi^\dagger \mathcal{M} \xi^\dagger) \mathcal{A}^\mu P_\mu^{*\dagger}(v) \\ + b P(v) \mathcal{A}^\mu (\xi \mathcal{M}^\dagger \xi + \xi^\dagger \mathcal{M} \xi^\dagger) P_\mu^{*\dagger}(v) + \text{H.c.} \end{aligned} \quad (2.12)$$

Obviously, in the above expression, we should take  $\xi = 1$  in  $(\xi \mathcal{M}^\dagger \xi + \xi^\dagger \mathcal{M} \xi^\dagger)$  in order to describe the decay  $P^* \rightarrow P \pi$ . As a consequence, the higher-order contribution due to (2.12) has the same structure as that of (2.11) except that the former vanishes in the chiral limit. As stressed in the Introduction, we will not consider higher-order Lagrangian effects in the present paper because of the unknown parameters  $a$  and  $b$  in (2.12). The sum of all chiral-loop contributions shown in Fig. 1 gives rise to the effective coupling constant

$$\begin{aligned} g_{\text{eff}} = & g \frac{\sqrt{Z_2(P) Z_2(P^*) Z_2(\pi^a)}}{Z_1} \\ = & g \frac{Z_2(P) \sqrt{Z_2(\pi^a)}}{Z_1}, \end{aligned} \quad (2.13)$$

where  $Z_1$  and  $Z_2$  are the vertex and wave-function renormalization constants, respectively, and the HQS relation  $Z_2(P^*) = Z_2(P)$  has been applied. For simplicity, wave-function renormalization and mass counterterms of the heavy meson and Goldstone boson are not explicitly shown in Fig. 1, but the usual mass renormalization procedure is to be understood. To evaluate the  $Z_2$  renormalization constant, we note that the self-energy amplitude of, for example,  $P_i$  has the expression

$$\begin{aligned} -i\Pi(\vec{k}) = & -\frac{g^2}{2f_0^2} M_P \\ & \times \sum_b (\lambda^b \lambda^b)_{ii} \\ & \times \int \frac{d^4 l}{(2\pi)^4} \frac{(g_{\mu\nu} - v_\mu v_\nu) l^\mu l^\nu}{(l^2 - m_{\pi^b}^2 + i\epsilon) [v \cdot (l + \vec{k}) + i\epsilon]}, \end{aligned} \quad (2.14)$$

where  $\vec{k}$  is the residual momentum defined by  $P_\mu = m_Q v_\mu + \vec{k}_\mu$  and  $m_{\pi^b}$  is the mass of the Goldstone bo-

son  $\pi^b$  in the loop. (For notation consistency we will follow papers I and II to denote the momenta of the Goldstone boson and photon by  $q$  and  $k$ , respectively.) With the help of Eq. (A4) and the relation

$$\Pi(\tilde{k}) = \delta m^2 - 2(Z_2^{-1} - 1)(v \cdot \tilde{k})M_P, \quad (2.15)$$

we obtain

$$\delta m^2(P_i) = -\frac{g^2}{16\pi} \sum_b (\lambda^b \lambda^b)_{ii} \frac{m_{\pi^b}^3}{f_0^2} M_{P_i} \quad (2.16)$$

and

$$Z_2(P_i) = 1 + \frac{3g^2}{64\pi^2} \sum_b (\lambda^b \lambda^b)_{ii} \frac{m_{\pi^b}^2}{f_0^2} \ln \frac{\Lambda^2}{m_{\pi^b}^2}, \quad (2.17)$$

where  $\Lambda$  is an arbitrary renormalization scale. As discussed in the Introduction, divergences from chiral loops are absorbed into the unrenormalized parameters of higher-derivative chiral Lagrangians, which are not written down here. It is straightforward to check that the HQS relation  $Z_2(P_i^*) = Z_2(P_i)$  holds. Note that the SU(3)-invariant masses  $M_P$  and  $M_{P^*}$  in Eq. (2.11) are unrenormalized masses; they are connected to the physical masses through the relations

$$\begin{aligned} M_{\text{phys}}^2(P_i) &= M_P^2 - 2\alpha_1 M_P \mathcal{M}_{ii} \\ &\quad - 2\alpha_3 M_P \text{tr} \mathcal{M} + \delta m^2(P_i), \\ M_{\text{phys}}^2(P_i^*) &= M_{P^*}^2 - 2\alpha_1 M_{P^*} \mathcal{M}_{ii} \\ &\quad - 2\alpha_3 M_{P^*} \text{tr} \mathcal{M} + \delta m^2(P_i^*). \end{aligned} \quad (2.18)$$

It follows from Eqs. (2.9), (2.16), and (2.18) that the mass splitting of, say,  $P_3 = (Q\bar{s})$  and  $P_1 = (Q\bar{u})$  is given by

$$\begin{aligned} M_{P_3}^{\text{phys}} - M_{P_1}^{\text{phys}} &= -\alpha_1(m_s - m_u) \\ &\quad - \frac{g^2}{32\pi} \sum_b [(\lambda^b \lambda^b)_{33} - (\lambda^b \lambda^b)_{11}] \frac{m_{\pi^b}^3}{f_0^2}. \end{aligned} \quad (2.19a)$$

Likewise, for heavy vector mesons,

$$M_{P_3^*}^{\text{phys}} - M_{P_1^*}^{\text{phys}} = M_{P_3}^{\text{phys}} - M_{P_1}^{\text{phys}}. \quad (2.19b)$$

Consequently, a measurement of the heavy meson mass differences will provide information on the parameter  $\alpha_1$ . We will come back to this in Sec. IV.

From the strong-interaction chiral Lagrangian for the Goldstone bosons,

$$\mathcal{L} = \frac{f_0^2}{4} \text{tr}(\partial_\mu \Sigma^\dagger \partial^\mu \Sigma) + \frac{f_0^2}{4} \text{tr}(\overline{\mathcal{M}}^\dagger \Sigma + \overline{\mathcal{M}} \Sigma^\dagger), \quad (2.20)$$

with  $\overline{\mathcal{M}} = \text{diag}(m_\pi^2, m_\pi^2, 2m_K^2 - m_\pi^2)$ , the wave-function renormalization constants for the light pseudoscalar mesons are found to be

$$\begin{aligned} \sqrt{Z_2(\pi)} &= 1 - \frac{1}{3}(2\epsilon_\pi + \epsilon_K), \\ \sqrt{Z_2(K)} &= 1 - \frac{1}{3}(\frac{3}{4}\epsilon_\pi + \frac{3}{2}\epsilon_K + \frac{3}{4}\epsilon_\eta), \\ \sqrt{Z_2(\eta)} &= 1 - \frac{1}{3}(3\epsilon_K), \end{aligned} \quad (2.21)$$

with

$$\begin{aligned} \epsilon_\pi &= \frac{1}{32\pi^2} \frac{m_\pi^2}{f_0^2} \ln \frac{\Lambda^2}{m_\pi^2}, \\ \epsilon_K &= \frac{1}{32\pi^2} \frac{m_K^2}{f_0^2} \ln \frac{\Lambda^2}{m_K^2}, \\ \epsilon_\eta &= \frac{1}{32\pi^2} \frac{m_\eta^2}{f_0^2} \ln \frac{\Lambda^2}{m_\eta^2}. \end{aligned} \quad (2.22)$$

As to the Feynman diagrams Figs. 1(a)–1(e), the amplitude of the vertex diagrams Figs. 1(a) and 1(b) reads

$$\begin{aligned} A(1(a)+1(b)) &= \frac{g^3}{64\pi^2} \sqrt{M_P M_{P^*}} \\ &\quad \times \sum_b (\lambda^b \lambda^a \lambda^b)_{ij} \frac{m_{\pi^b}^2}{f_0^3} \ln \frac{\Lambda^2}{m_{\pi^b}^2} (\epsilon^* \cdot q), \end{aligned} \quad (2.23)$$

where we have applied Eq. (A3). To evaluate the seagull graphs of Figs. 1(c) and 1(d), we note that the Feynman rules for the vertices  $PP\pi^a\pi^b$  and  $P^*P^*\pi^a\pi^b$  are obtained from the kinematic terms in Eq. (2.1) together with Eqs. (2.3)–(2.6) and

$$\mathcal{V}_\mu = \frac{1}{4f_0} (M \partial_\mu M - \partial_\mu M M) + \dots, \quad (2.24)$$

where  $M$  is the meson matrix given by Eq. (2.4). The relevant Feynman rules are

$$-\frac{i}{4f_0^2} M_P (\lambda^a \lambda^b - \lambda^b \lambda^a) v \cdot (q_a - q_b) \quad (2.25)$$

for the vertex  $PP\pi^a\pi^b$  and

$$\frac{i}{4f_0^2} M_{P^*} (\lambda^a \lambda^b - \lambda^b \lambda^a) v \cdot (q_a - q_b) (\epsilon^* \cdot \epsilon'^*) \quad (2.26)$$

for  $P^*P^*\pi^a\pi^b$ . Therefore both vertices are proportional to  $v \cdot (q_a - q_b)$ . As a consequence, seagull diagrams Figs. 1(c) and 1(d) vanish since the required  $\epsilon^* \cdot q$  expression cannot be generated from the seagull amplitudes in which the linear  $q$  dependence is always in the  $v \cdot q$  form. Beyond the heavy quark limit, seagull graphs do contribute, but they are suppressed by factors of  $1/M_{P^*}$  relative to the tree amplitude. For example, to order  $1/M_{P^*}$ , the  $P^*P^*\pi^a\pi^b$  vertex

$$\begin{aligned} &-\frac{i}{8f_0^2} (\lambda^a \lambda^b - \lambda^b \lambda^a) M_P [(q_a - q_b) \cdot \epsilon'^* (v \cdot \epsilon^*) \\ &\quad - (q_a - q_b) \cdot \epsilon^* (v \cdot \epsilon'^*)] \end{aligned}$$

is no longer vanishing as  $v \cdot \epsilon^* \neq 0$  and  $v \cdot \epsilon'^* \neq 0$ .

The five-point vertex in Fig. 1(e) is generated from the Lagrangian (2.1) by expanding  $\mathcal{A}_\mu$  to the third power of  $M$ :

$$\begin{aligned} \mathcal{A}_\mu = & -\frac{1}{\sqrt{2}f_0} \partial_\mu M \\ & + \frac{1}{12\sqrt{2}f_0^3} [(\partial_\mu M)M^2 - 2M(\partial_\mu M)M \\ & + M^2 \partial_\mu M] + \dots \end{aligned} \quad (2.27)$$

A straightforward calculation shows that the contribution due to the five-point vertex diagram Fig. 1(e) is exactly compensated by the wave-function renormalization of the Goldstone bosons. As a consequence, we have effectively

$$g_{\text{eff}} = g \frac{Z_2(P)}{Z_1(1(a)+1(b))}, \quad (2.28)$$

with

$$Z_1(1(a)+1(b)) = 1 - \frac{g^2}{2} \sum_b \frac{(\lambda^b \lambda^a \lambda^b)_{ij}}{(\lambda^a)_{ij}} \epsilon_{\pi^b}. \quad (2.29)$$

It follows from Eq. (2.17) that the individual wave-function renormalization constants for heavy mesons are given by

$$\begin{aligned} Z_2(P_1) = Z_2(P_2) &= 1 + g^2 \left( \frac{3}{2} \epsilon_\pi + 3\epsilon_K + \frac{1}{2} \epsilon_\eta \right), \\ Z_2(P_3) &= 1 + 2g^2 (3\epsilon_K + \epsilon_\eta). \end{aligned} \quad (2.30)$$

In Sec. IV the above results will be applied to the strong decay  $D^* \rightarrow D + \pi$ . There we shall see that  $Z_2$  plays an essential role and the pion contribution is not negligible in spite of its small mass.

Thus far we have expressed all the results in terms of the unrenormalized decay constant  $f_0$ . It can be related to the physical decay constants through the relations [16]

$$\begin{aligned} f_\pi &= f_0 \left[ 1 + 2\epsilon_\pi + \epsilon_K + 4 \frac{2m_K^2 + m_\pi^2}{f_0^2} L_4^r + 4 \frac{m_\pi^2}{f_0^2} L_5^r \right], \\ f_K &= f_0 \left[ 1 + \frac{3}{4} \epsilon_\pi + \frac{3}{2} \epsilon_K + \frac{3}{4} \epsilon_\eta + 4 \frac{2m_K^2 + m_\pi^2}{f_0^2} L_4^r \right. \\ &\quad \left. + 2 \frac{m_\pi^2}{f_0^2} \frac{m_s + \hat{m}}{\hat{m}} L_5^r \right], \quad (2.31) \\ f_\eta &= f_0 \left[ 1 + 3\epsilon_K + 4 \frac{2m_K^2 + m_\pi^2}{f_0^2} L_4^r + \frac{4}{3} \frac{m_\pi^2}{f_0^2} \frac{2m_s + \hat{m}}{\hat{m}} L_5^r \right], \end{aligned}$$

where  $\hat{m} = (m_u + m_d)/2$  and the counterterm contributions denoted by the renormalized coupling constants  $L_4^r$  and  $L_5^r$  (see Ref. [16] for notation) are included in Eq. (2.31). Note that the one-loop logarithmic corrections to the decay constants, the pion wave-function renormalization, and the five-point vertex diagram all share the same structure as they come from the same chiral-loop diagram. The couplings  $L_4^r$  and  $L_5^r$  of the four-derivative chiral Lagrangian are dependent on the renormalization scale  $\Lambda$ . However, physical decay constants can be verified to be independent of the choice of  $\Lambda$ , as they

should be [16]. Using the empirical values

$$\begin{aligned} L_4^r(\Lambda = m_\eta) &= (0 \pm 0.5) \times 10^{-3}, \\ L_5^r(\Lambda = m_\eta) &= (2.2 \pm 0.5) \times 10^{-3}, \end{aligned} \quad (2.32)$$

obtained in Ref. [16], and the experimental value  $f_\pi = 93$  MeV [21] we find

$$f_0 \simeq 86 \text{ MeV}. \quad (2.33)$$

We make a digression here to comment on the  $1/m_Q$  effects. In the heavy quark effective theory,  $1/m_Q$  corrections can be systematically studied by including the following higher-dimensional operators

$$O_1 = \frac{1}{2m_Q} \bar{h}_v^{(Q)} (iD)^2 h_v^{(Q)}, \quad (2.34)$$

$$O_2 = \frac{1}{2m_Q} \bar{h}_v^{(Q)} \left( -\frac{1}{2} g_s \sigma_{\mu\nu} G^{\mu\nu} \right) h_v^{(Q)},$$

where  $h_v^{(Q)}$  is a velocity-dependent heavy quark field. For the case of  $P^* \rightarrow P\pi$  decays, there are two different kinds of  $1/m_Q$  corrections. One arises from the consideration of the subleading decay amplitude induced by the operators  $O_1$  and  $O_2$ . As shown in the preceding paper [13], the coupling constant  $g$  receives a correction of order  $\Lambda_{\text{QCD}}/m_Q$ ; that is,

$$g_{\text{eff}} = g \left[ 1 + O \left[ \frac{\Lambda_{\text{QCD}}}{m_Q} \right] \right]. \quad (2.35)$$

This  $1/m_Q$  effect in the chiral limit is elaborated on in more details in Ref. [13]. The other kind of  $1/m_Q$  correction comes from the combination of chiral symmetry and heavy flavor symmetry breakings, e.g., the seagull diagrams. Schematically, it is expected to be the order of

$$\frac{1}{(4\pi)^2} \frac{m_{\pi^b}^2}{f_0^2} \frac{m_{\pi^b}}{m_Q}, \quad (2.36)$$

where the factor  $1/(4\pi)^2$  is associated with the loop-momentum integration and  $m_{\pi^b}$  is the mass of the loop meson  $\pi^b$ . As this SU(3)-violating  $1/m_Q$  effect is very small, we will not pursue it further.

We next turn to the electromagnetic decay of heavy mesons. One-loop contributions to  $P^* \rightarrow P + \gamma$  are shown in Fig. 2. The Feynman diagrams with a photon coupled to the external  $P^*$  or  $P$  line via charge coupling are vanishing, as expected since the reaction under consideration involves a magnetic  $M1$  transition. Therefore they are not displayed in Fig. 2. Although chiral-loop effects in the radiative decays have been recently discussed by Amundson *et al.* [8], only Fig. 2(e) was analyzed by them. Before proceeding to compute loop corrections, we note that the tree amplitude obtained from (2.2) is

$$A [P_i^*(v, \epsilon^*) \rightarrow P_i + \gamma(k, \epsilon)] = \rho_i \epsilon_{\mu\nu\alpha\beta} k^\mu \epsilon^\nu v^\alpha \epsilon^{*\beta}, \quad (2.37)$$

with

$$\begin{aligned} \rho_i &= -2\sqrt{M_P M_{P^*}} (e_i d + e_Q d') \\ &= e\sqrt{M_P M_{P^*}} (e_i \beta + e_Q \beta') \end{aligned} \quad (2.38)$$

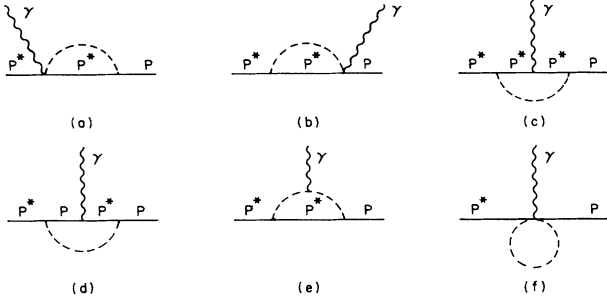


FIG. 2. Chiral-loop diagrams contributing to the radiative decay  $P^* \rightarrow P\gamma$ .

and  $e_i = Q_{ii}$ . Though the unknown parameter  $\beta \equiv -2d/e$  is not fixed by heavy quark symmetry, the other parameter  $\beta' \equiv -2d'/e$  is determined in the heavy quark effective theory by the dimension-5 operator

$$O_3 = \frac{1}{2m_Q} \bar{h}_v^{(Q)} \left( -\frac{1}{2} e e_Q \sigma_{\mu\nu} F^{\mu\nu} \right) h_v^{(Q)}, \quad (2.39)$$

with the result [7,8,10]

$$\beta' = \frac{1}{m_Q}. \quad (2.40)$$

It should be stressed that it is important to include this  $1/m_Q$  effect due to the magnetic moment of the heavy quark. As we have seen in paper II, the charmed quark contribution is significant and largely destructive in the radiative decays of  $D^{*+}$  and  $D_s^{*+}$ . In the nonrelativistic quark model,  $\beta$  is related to the constituent quark mass, namely,  $\beta = 1/M_q$  [10]. Since in the spirit of chiral perturbation theory SU(3) violation is induced by chiral-symmetry-breaking terms, it is interesting to compare the quark model results with those of the chiral Lagrangian approach. To the lowest order, it is evident that  $\rho_2 = \rho_3$  or

$$A(P_2^* \rightarrow P_2\gamma) = A(P_3^* \rightarrow P_3\gamma). \quad (2.41)$$

As will be seen, this SU(3) relation is badly broken by chiral-loop effects.

Referring to Fig. 2 the effective couplings become

$$\begin{aligned} (\beta_i)_{\text{eff}} &= \beta \frac{Z_2(P_i)}{(Z_1)_i} + \delta\beta_i(2(a)+2(b)+2(e)), \\ (\beta'_i)_{\text{eff}} &= \beta' \frac{Z_2(P_i)}{(Z'_1)_i}, \end{aligned} \quad (2.42)$$

where the subscript  $i$  refers to the process  $P_i^* \rightarrow P_i\gamma$  and  $Z_1$  accounts for the vertex renormalization due to Figs. 2(c), 2(d), and 2(f). We begin with Fig. 2(e). In order to evaluate its amplitude, all the charged meson loops are

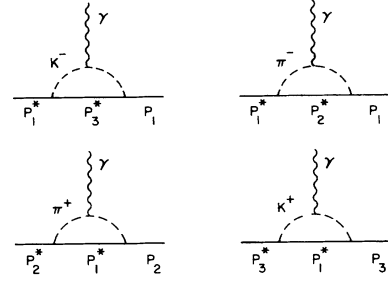


FIG. 3. Amplification of Fig. 2(e) with all charged meson loops specified.

explicitly shown in Fig. 3. By virtue of Eq. (A2), we find<sup>4</sup>

$$\begin{aligned} \delta\beta_1(2(e)) &= \frac{1}{e_1} \left[ -\frac{g^2 m_\pi}{8\pi f_0^2} - \frac{g^2 m_K}{8\pi f_0^2} \right], \\ \delta\beta_2(2(e)) &= \frac{1}{e_2} \left[ \frac{g^2 m_\pi}{8\pi f_0^2} \right], \\ \delta\beta_3(2(e)) &= \frac{1}{e_3} \left[ \frac{g^2 m_K}{8\pi f_0^2} \right], \end{aligned} \quad (2.43)$$

which are in agreement with Ref. [8]. As for the seagull diagrams Figs. 2(a) and 2(b), we note that the electromagnetic four-point interactions of heavy mesons are described by

$$\begin{aligned} & \frac{-\sqrt{2}eg}{f_0} \epsilon^{\mu\nu\lambda\kappa} A_\mu v_\nu P_\lambda^*(v) [Q, M] P_\kappa^{*\dagger}(v) \\ & - i\sqrt{M_P M_{P^*}} \frac{\sqrt{2}eg}{f_0} A^\mu \\ & \times \{ P(v) [Q, M] P_\mu^{*\dagger}(v) + P_\mu^*(v) [Q, M] P^\dagger(v) \}, \end{aligned} \quad (2.44)$$

where use has been made of

$$\begin{aligned} \mathcal{A}_\mu &= \mathcal{A}_\mu^{(0)} - \frac{1}{2} e A_\mu (\xi^\dagger Q \xi - \xi Q \xi^\dagger) \\ &= -\frac{1}{\sqrt{2}f_0} \partial_\mu M - \frac{ie}{\sqrt{2}f_0} A_\mu [Q, M] + \dots \end{aligned} \quad (2.45)$$

in (2.1) and (2.2). It is clear that the  $P^*P\pi^a\gamma$  vertex is independent of the photon's momentum  $k$ . As a consequence, Fig. 2(b) with a photon emitted from the vertex on the right-hand side (RHS) does not contribute since no linear  $k$ -dependent terms can be constructed from the numerator or the denominator after the loop momenta of the  $\pi^b$  and  $P^*$  are assigned to be  $l$  and  $p+l$ , respectively. Since the vertex  $P^*P^*\pi^a\gamma$  is proportional to  $\epsilon^{\mu\nu\lambda\kappa} v_\mu \epsilon_{\nu\lambda}^* \epsilon_\kappa^*$  in the heavy quark limit, it is easily seen that the other seagull diagram Fig. 2(a) also vanishes. Its

<sup>4</sup>In Ref. [8],  $f_0$  is replaced by the physical decay constant  $f_\pi$  for the pion loop and  $f_K$  for the kaon loop. We will not make such a replacement in our calculation.

subleading contribution is of order  $(g^2/f_0^2)(1/M_{P^*})$  and hence negligible.

We next focus on vertex corrections. With the magnetic  $P^*P\gamma$  and  $P^*P^*\gamma$  vertices determined from (2.2), Figs. 2(c) and 2(d) lead to

$$Z_1(P_i^* \rightarrow P_i\gamma; 2(c)+2(d)) = 1 - \frac{g^2}{2} \sum_b \frac{(\lambda^b Q \lambda^b)_{ii}}{Q_{ii}} \epsilon_{\pi^b} \quad (2.46)$$

and

$$Z'_1(P_i^* \rightarrow P_i\gamma; 2(c)+2(d)) = Z_2(P_i), \quad (2.47)$$

where we have applied (2.17) and the relations (2.7) and (2.8). The contribution of Fig. 2(c) due to charge  $P^*P^*\gamma$  coupling is of order  $(g^2/32\pi^2)(m_{\pi^b}^2/f_0^2)(m_{\pi^b}/M_P)$  and hence negligible. Note that because  $Z'_1(P_i^* \rightarrow P_i\gamma)$  is exactly compensated by  $Z_2(P_i)$ , the parameter  $\beta'$  of (2.42) does not get renormalized; this is a realization in chiral perturbation theory of the exact QCD result discussed in Ref. [13].

It remains to compute the amplitude of Fig. 2(f). The relevant electromagnetic five-point vertex obtained from (2.2) is

$$-\frac{d}{2f_0^2} \sqrt{M_P M_{P^*}} \epsilon_{\mu\nu\alpha\beta} k^\mu \epsilon^\nu v^\alpha \epsilon^{*\beta} [M, [Q, M]]. \quad (2.48)$$

It is easily seen that only charged meson loops contribute; the result is

$$Z_1(P_i^* \rightarrow P_i\gamma; 2(f)) = 1 + \frac{1}{4} \sum_b [\lambda^b, [Q, \lambda^b]]_{ii} \frac{\epsilon_{\pi^b}}{Q_{ii}}. \quad (2.49)$$

Working out (2.46) and (2.49) explicitly, we find the total vertex corrections to be

$$\begin{aligned} Z_1(P_1^* \rightarrow P_1\gamma; 2(c)+2(d)+2(f)) \\ = 1 + \frac{1}{e_1} \left[ -\epsilon_\pi - \epsilon_K + \frac{g^2}{3} \left[ \epsilon_K - \frac{1}{3} \epsilon_\eta \right] \right], \\ Z_1(P_2^* \rightarrow P_2\gamma; 2(c)+2(d)+2(f)) \\ = 1 + \frac{1}{e_2} \left[ \epsilon_\pi + \frac{g^2}{3} \left[ -\frac{3}{2} \epsilon_\pi + \epsilon_K + \frac{1}{6} \epsilon_\eta \right] \right], \quad (2.50) \end{aligned}$$

$$\begin{aligned} Z_1(P_3^* \rightarrow P_3\gamma; 2(c)+2(d)+2(f)) \\ = 1 + \frac{1}{e_3} \left[ \epsilon_K + \frac{g^2}{3} \left[ -\epsilon_K + \frac{2}{3} \epsilon_\eta \right] \right]. \end{aligned}$$

Putting everything together, we obtain the following effective couplings for  $P_i^* \rightarrow P_i\gamma$ :

$$\begin{aligned} \rho_1 &= e \sqrt{M_P M_{P^*}} \left[ \frac{2}{3} \beta \frac{Z_2(P_1)}{Z_1(P_1^* \rightarrow P_1\gamma)} \right. \\ &\quad \left. + \frac{e_Q}{m_Q} - \frac{g^2}{8\pi} \frac{m_\pi}{f_0^2} - \frac{g^2}{8\pi} \frac{m_K}{f_0^2} \right], \\ \rho_2 &= e \sqrt{M_P M_{P^*}} \left[ -\frac{1}{3} \beta \frac{Z_2(P_2)}{Z_1(P_2^* \rightarrow P_2\gamma)} \right. \\ &\quad \left. + \frac{e_Q}{m_Q} + \frac{g^2}{8\pi} \frac{m_\pi}{f_0^2} \right], \quad (2.51) \\ \rho_3 &= e \sqrt{M_P M_{P^*}} \left[ -\frac{1}{3} \beta \frac{Z_2(P_3)}{Z_1(P_3^* \rightarrow P_3\gamma)} \right. \\ &\quad \left. + \frac{e_Q}{m_Q} + \frac{g^2}{8\pi} \frac{m_K}{f_0^2} \right]. \end{aligned}$$

In the SU(3) limit, the light quark contributions to  $\rho$  are in the ratio 2:−1:−1 for the electromagnetic decays of  $P_1^*$ ,  $P_2^*$ , and  $P_3^*$ . Evidently, this relation is violated by the wave-function and vertex renormalizations.

### III. SU(3)-SYMMETRY-BREAKING CORRECTIONS TO THE CHIRAL DYNAMICS OF HEAVY BARYONS

In this section we discuss the corrections to the strong and radiative decays of heavy baryons containing a heavy quark  $Q$  and two light quarks. The two light quarks form either a symmetric sextet  $\mathbf{6}$  or an antisymmetric antitriplet  $\bar{\mathbf{3}}$  in flavor SU(3) space. We will denote these spin- $\frac{1}{2}$  baryons as  $B_6$  and  $B_{\bar{3}}$ , respectively, and the spin- $\frac{3}{2}$  baryon by  $B_6^*$ . Explicitly, the baryon matrices read as in paper I:

$$B_{\bar{3}} = \begin{pmatrix} 0 & \Lambda_Q & \Xi_Q^{1/2} \\ -\Lambda_Q & 0 & \Xi_Q^{-1/2} \\ -\Xi_Q^{1/2} & -\Xi_Q^{-1/2} & 0 \end{pmatrix}, \quad (3.1)$$

$$B_6 = \begin{pmatrix} \Sigma_Q^+ & \frac{1}{\sqrt{2}} \Sigma_Q^0 & \frac{1}{\sqrt{2}} \Xi_Q'^{1/2} \\ \frac{1}{\sqrt{2}} \Sigma_Q^0 & \Sigma_Q^- & \frac{1}{\sqrt{2}} \Xi_Q'^{-1/2} \\ \frac{1}{\sqrt{2}} \Xi_Q'^{1/2} & \frac{1}{\sqrt{2}} \Xi_Q'^{-1/2} & \Omega_Q \end{pmatrix}, \quad (3.2)$$

and a matrix for  $B_6^*$  similar to  $B_6$ . The superscript in (3.1) and (3.2) refers to the value of the isospin quantum number  $I_3$ .

To perform chiral-loop calculations, we find that for sextet heavy baryons it is very convenient to work with the ‘‘superfields’’ which combine spin- $\frac{1}{2}$  and spin- $\frac{3}{2}$  sextet baryon fields into a single field [6,17],

$$\begin{aligned} S^\mu &= B_6^{*\mu} - \frac{1}{\sqrt{3}} (\gamma^\mu + v^\mu) \gamma_5 B_6, \\ \bar{S}^\mu &= \bar{B}_6^{*\mu} + \frac{1}{\sqrt{3}} \bar{B}_6 \gamma_5 (\gamma^\mu + v^\mu), \end{aligned} \quad (3.3)$$

where  $B_{6\mu}^*$  is the Rarita-Schwinger vector-spinor field as appropriate for spin- $\frac{3}{2}$  particles. Feynman rules in terms of superfields become much simpler, and there are fewer Feynman diagrams to evaluate. The most general gauge-invariant chiral Lagrangian for heavy baryons given by Eq. (II.3.8) reads

$$\begin{aligned} \mathcal{L}_B^{(1)} = & -i \operatorname{tr}(\bar{S}^\mu v \cdot DS_\mu) + \frac{i}{2} \operatorname{tr}(\bar{T}v \cdot DT) + \Delta m \operatorname{tr}(\bar{S}^\mu S_\mu) \\ & + i\frac{3}{2}g_1 \epsilon_{\mu\alpha\beta\nu} \operatorname{tr}(\bar{S}^\mu v^\alpha \mathcal{A}^\beta S^\nu) \\ & - \sqrt{3}g_2 \operatorname{tr}(\bar{S}^\mu \mathcal{A}_\mu T) + \text{H.c.} \end{aligned} \quad (3.4)$$

in superfield notation, where  $T \equiv B_{\bar{3}}$  and  $\Delta m$  is the mass splitting between the sextet and antitriplet baryon multiplets (for simplicity we will drop the unknown  $\Delta m$  term in ensuing loop calculations). We wish to stress that the Lagrangian (3.4) is expressed in terms of velocity-dependent baryon fields. Because of heavy quark symmetry, there are only two independent coupling constants in the low-energy interactions between the Goldstone bosons and heavy baryons. Moreover, the nonrelativistic quark model predicts that [3]

$$g_1 = \frac{1}{3}g, \quad g_2 = -\left(\frac{2}{3}\right)^{1/2}g, \quad (3.5)$$

with  $g$  being the axial-vector coupling constant of a constituent quark, which is also the coupling constant appearing in the meson Lagrangian (2.1). Feynman rules can be easily derived from (3.4). Especially, the  $S$  and  $T$  propagators are simply given by  $i(-g_{\mu\nu} + v_\mu v_\nu)/(v \cdot \tilde{k} - \Delta m)$  and  $i/v \cdot \tilde{k}$ , respectively, where  $\tilde{k}$  is the residual momentum of the heavy hadron. The lowest-order chiral-symmetry-breaking terms now have the form

$$\begin{aligned} \mathcal{L}_{\text{CSB}} = & \lambda_1 \operatorname{tr}[\bar{S}^\mu (\xi \mathcal{M}^\dagger \xi + \xi^\dagger \mathcal{M} \xi^\dagger) S_\mu] \\ & + \lambda_2 \operatorname{tr}(\bar{S}^\mu S_\mu) \operatorname{tr}(\mathcal{M}^\dagger \Sigma + \Sigma^\dagger \mathcal{M}) \\ & + \lambda_3 \operatorname{tr}[\bar{T} (\xi \mathcal{M}^\dagger \xi + \xi^\dagger \mathcal{M} \xi^\dagger) T] \\ & + \lambda_4 \operatorname{tr}(\bar{T} T) \operatorname{tr}(\mathcal{M}^\dagger \Sigma + \Sigma^\dagger \mathcal{M}). \end{aligned} \quad (3.6)$$

We begin by first examining the chiral-loop effects on the strong decays  $B_Q \rightarrow B_Q' + \pi^a$ . The tree amplitudes of  $S_{ij} \rightarrow S_{ij} + \pi^a$  and  $S_{ij} \rightarrow T_{ij} + \pi^a$  derived from (3.4) are

$$\begin{aligned} A[S_{ij}^\mu(v) \rightarrow S_{ij}^\nu \pi^a(q)] \\ = i \frac{3}{8} \frac{g_1}{f_0} \bar{u}^\nu \epsilon_{\nu\alpha\beta\mu} v^\alpha q^\beta (\lambda_{ii}^a + \lambda_{jj}^a) \mathcal{U}^\mu, \end{aligned} \quad (3.7)$$

$$\begin{aligned} A[S_{ij}^\mu(v) \rightarrow T_{ij} \pi^a(q)] \\ = -\frac{\sqrt{3}}{2\sqrt{2}} \frac{g_2}{f_0} \bar{u}_3 q_\mu (\lambda_{ii}^a - \lambda_{jj}^a) \mathcal{U}^\mu \quad (i < j), \end{aligned}$$

with  $\mathcal{U}_\mu = u_\mu - (1/\sqrt{3})(\gamma_\mu + v_\mu)\gamma_5 u$ . It is a simple matter to project out from (3.7) the strong decay amplitudes expressed in terms of component fields  $B_6^*, B_6, B_{\bar{3}}$ . For example, Eq. (3.7) leads to

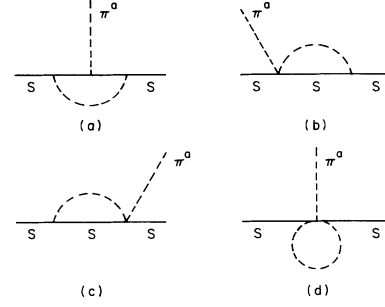


FIG. 4. Chiral-loop diagrams contributing to the strong decay  $S \rightarrow S\pi^a$ . In (a), the external pion may originate from an  $SS\pi$  or  $ST\pi$  vertex.

$$\begin{aligned} A[(B_6^{*\mu})_{ij} \rightarrow (B_6)_{ij} \pi^a(q)] &= \frac{\sqrt{3}}{8} \frac{g_1}{f_0} \bar{u}_6 q_\mu (\lambda_{ii}^a + \lambda_{jj}^a) u^\mu, \\ A[(B_6)_{ij} \rightarrow (B_{\bar{3}})_{ij} \pi^a(q)] \\ &= \frac{g_2}{2\sqrt{2}f_0} \bar{u}_3 \not{q} \gamma_5 (\lambda_{ii}^a - \lambda_{jj}^a) u_6 \quad (i < j). \end{aligned} \quad (3.8)$$

One-loop contributions are shown in Figs. 4 and 5, respectively, for  $S \rightarrow S\pi$  and  $S \rightarrow T\pi$ . The resultant effective couplings are given by

$$(g_1)_{\text{eff}} = g_1 \frac{Z_2(S) \sqrt{Z_2(\pi^a)}}{Z_1} \quad (3.9)$$

and

$$(g_2)_{\text{eff}} = g_2 \frac{\sqrt{Z_2(S)Z_2(T)Z_2(\pi^a)}}{Z_1'}, \quad (3.10)$$

where  $Z_2(T)$  and  $Z_2(S)$  are, respectively, the wavefunction renormalization constants for  $T$  and  $S$  baryon fields and  $Z_1$  and  $Z_1'$  account for vertex renormalization effects from Figs. 4(a)–4(d) and 5(a)–5(d), respectively.

To evaluate the renormalization constant  $Z_2$ , we note that the self-energy amplitudes can be written as  $-i\Sigma(\tilde{k})$  and  $i\Sigma(\tilde{k})g_{\mu\nu}$  for  $T$  and  $S$  heavy baryon fields, respectively. Since

$$\Sigma(\tilde{k}) = \delta m - (Z_2^{-1} - 1)v \cdot \tilde{k}, \quad (3.11)$$

we find<sup>5</sup>

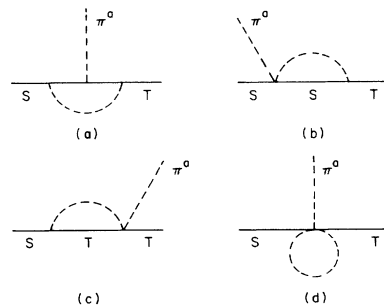


FIG. 5. Chiral-loop diagrams contributing to the strong decay  $S \rightarrow T\pi^a$ . In (a), the external pion may originate from an  $SS\pi$  or  $ST\pi$  vertex.

<sup>5</sup>Our results for  $Z_2(T)$  and  $Z_2(S)$  [see also Eq. (3.15)] disagree with Eq. (3.3) of Ref. [17].

$$\begin{aligned}\delta m(T_{ij}) &= -\frac{3}{32\pi} g_2^2 \sum_b \frac{1}{2} [(\lambda^b \lambda^b)_{ii} + (\lambda^b \lambda^b)_{jj} + 2\lambda_{ij}^b \lambda_{ji}^b - 2\lambda_{ii}^b \lambda_{jj}^b] \frac{m_{\pi^b}^3}{f_0^2}, \\ Z_2(T_{ij}) &= 1 + \frac{9}{8} g_2^2 \sum_b \frac{1}{2} [(\lambda^b \lambda^b)_{ii} + (\lambda^b \lambda^b)_{jj} + 2\lambda_{ij}^b \lambda_{ji}^b - 2\lambda_{ii}^b \lambda_{jj}^b] \epsilon_{\pi^b} \quad (i \neq j),\end{aligned}\tag{3.12}$$

for the antitriplet baryon  $B_{\bar{3}}$  with the  $\epsilon_{\pi^b}$ 's being defined in (2.22). Likewise, we get

$$\begin{aligned}\delta m(S_{ij}) &= -\frac{1}{128\pi} \sum_b (6g_1^2 \xi_{ij}^s + 4g_2^2 \zeta_{ij}^s) \frac{m_{\pi^b}^3}{f_0^2}, \\ Z_2(S_{ij}) &= 1 + \frac{3}{8} \sum_b (6g_1^2 \xi_{ij}^s + 4g_2^2 \zeta_{ij}^s) \epsilon_{\pi^b},\end{aligned}\tag{3.13}$$

for the sextet baryons  $B_6$  and  $B_6^*$ , where

$$\begin{aligned}\xi_{ij}^s &= \frac{1}{4} [(\lambda^b \lambda^b)_{ii} + (\lambda^b \lambda^b)_{jj} + 2\lambda_{ij}^b \lambda_{ji}^b + 2\lambda_{ii}^b \lambda_{jj}^b (1 - \delta_{ij})], \\ \zeta_{ij}^s &= \frac{1}{2} [(\lambda^b \lambda^b)_{ii} + (\lambda^b \lambda^b)_{jj} - 2\lambda_{ij}^b \lambda_{ji}^b - 2\lambda_{ii}^b \lambda_{jj}^b (1 - \delta_{ij})].\end{aligned}\tag{3.14}$$

It follows from Eqs. (3.12) and (3.13) that

$$\begin{aligned}Z_2(\Lambda_Q) &= 1 + 9g_2^2 (3\epsilon_\pi + \epsilon_K), \\ Z_2(\Xi_Q) &= 1 + \frac{9}{4} g_2^2 (3\epsilon_\pi + 10\epsilon_K + 3\epsilon_\eta), \\ Z_2(\Sigma_Q) &= 1 + \frac{9}{8} g_1^2 (4\epsilon_\pi + 2\epsilon_K + \frac{2}{3}\epsilon_\eta) + 3g_2^2 (\epsilon_\pi + \epsilon_K), \\ Z_2(\Xi'_Q) &= 1 + \frac{9}{8} g_1^2 (\frac{3}{2}\epsilon_\pi + 5\epsilon_K + \frac{1}{6}\epsilon_\eta) + \frac{3}{4} g_2^2 (3\epsilon_\pi + 2\epsilon_K + 3\epsilon_\eta), \\ Z_2(\Omega_Q) &= 1 + \frac{9}{8} g_1^2 (4\epsilon_K + \frac{8}{3}\epsilon_\eta) + 6g_2^2 \epsilon_K.\end{aligned}\tag{3.15}$$

As for the vertex diagram Fig. 4(a) for  $S_{ij} \rightarrow S_{ij} + \pi$  (since mass differences are generally small among different spin multiplets of heavy baryons, we will thus only consider pion emission due to the small phase space), the general expression is

$$Z_1(4(a)) = 1 + \sum_b \left( \frac{9}{4} g_1^2 \xi_{ij} - 6g_2^2 \zeta_{ij} \right) \frac{\epsilon_{\pi^b}}{\lambda_{ii}^3 + \lambda_{jj}^3},\tag{3.16}$$

with [see Appendix B for a derivation of the SU(3) group factors]

$$\begin{aligned}\xi_{ij} &= \frac{1}{8} \{ (\lambda^b \lambda^3 \lambda^b)_{jj} + \lambda_{ii}^3 (\lambda^b \lambda^b)_{jj} + \lambda_{ji}^b (\lambda^3 \lambda^b)_{ij} + (\lambda^b \lambda^3)_{ji} \lambda_{ij}^b + [\lambda_{ij}^3 (\lambda^b \lambda^b)_{ji} + (\lambda^b \lambda^3)_{jj} \lambda_{ii}^b + \lambda_{jj}^b (\lambda^3 \lambda^b)_{ii}] (1 - \delta_{ij}) + (i \leftrightarrow j) \}, \\ \zeta_{ij} &= \frac{1}{4} \{ (\lambda^b \lambda^3 \lambda^b)_{jj} - \lambda_{ii}^3 (\lambda^b \lambda^b)_{jj} - \lambda_{ij}^3 (\lambda^b \lambda^b)_{ji} (1 - \delta_{ij}) + (i \leftrightarrow j) \}.\end{aligned}\tag{3.17}$$

Note that  $Z_1$  in Eq. (3.16) is worked out for  $\pi^0$  emission, but due to SU(2) symmetry it should be also valid for charged pion emission. We next express the vertex corrections explicitly for  $S(\Sigma_Q^{(*)}) \rightarrow S(\Sigma_Q)\pi$  and  $S(\Xi_Q^{(*)}) \rightarrow S(\Xi'_Q)\pi$ :

$$Z_1(4(a)) = 1 + \left( \frac{9}{8} g_1^2 + 6g_2^2 \right) (\epsilon_\pi + \frac{1}{2}\epsilon_K) + \frac{3}{8} g_1^2 \epsilon_\eta\tag{3.18}$$

for  $S(\Sigma_Q^{(*)}) \rightarrow S(\Sigma_Q)\pi$  and

$$Z_1(4(a)) = 1 + \frac{9}{8} g_1^2 \left( -\frac{1}{4}\epsilon_\pi + 2\epsilon_K + \frac{1}{12}\epsilon_\eta \right) + 6g_2^2 \left( \frac{1}{4}\epsilon_\pi + \epsilon_K + \frac{1}{4}\epsilon_\eta \right)\tag{3.19}$$

for  $S(\Xi_Q^{(*)}) \rightarrow S(\Xi'_Q)\pi$ . Similarly, for  $S_{ij} \rightarrow T_{ij} + \pi$ , Fig. 5(a) leads to

$$Z_1'(5(a)) = 1 + \sum_b \left[ -\frac{9}{2\sqrt{2}} g_1^2 \xi'_{ij} + \frac{3}{\sqrt{2}} g_2^2 \zeta'_{ij} \right] \frac{\epsilon_{\pi^b}}{\lambda_{ii}^3 - \lambda_{jj}^3} \quad (i < j),\tag{3.20}$$

with

$$\begin{aligned}\xi'_{ij} &= \frac{1}{4\sqrt{2}} \{ (\lambda^b \lambda^3 \lambda^b)_{ii} + \lambda_{jj}^3 (\lambda^b \lambda^b)_{ii} + \lambda_{ij}^b (\lambda^3 \lambda^b)_{ji} + (\lambda^b \lambda^3)_{ij} \lambda_{ji}^b - (i \leftrightarrow j) \}, \\ \zeta'_{ij} &= \frac{1}{2\sqrt{2}} \{ (\lambda^b \lambda^3 \lambda^b)_{ii} - \lambda_{jj}^3 (\lambda^b \lambda^b)_{ii} + \lambda_{ii}^b (\lambda^3 \lambda^b)_{jj} - (\lambda^b \lambda^3)_{ii} \lambda_{jj}^b - (i \leftrightarrow j) \}.\end{aligned}\tag{3.21}$$

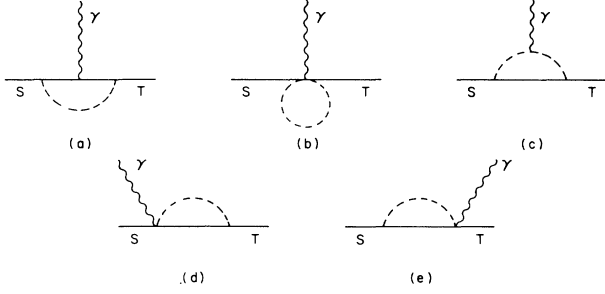


FIG. 6. Chiral-loop diagrams contributing to the radiative decay  $S \rightarrow S\gamma$ . In (a), the photon may originate from an  $SS\gamma$ ,  $ST\gamma$ , or  $TT\gamma$  vertex with a coupling constant  $a_1$ ,  $a_2$ , or  $a'_1$ . In (c), (d), and (e), the intermediate state can be an  $S$  or  $T$  baryon. A diagram similar to (b) but with a photon attached to the light meson does not contribute to the  $M1$  transition of  $S \rightarrow S\gamma$ .

Explicitly,

$$Z'_1(5(a)) = 1 + \frac{9}{2}g_1^2(\epsilon_\pi + \frac{1}{4}\epsilon_K) + 3g_2^2(\epsilon_\pi + \frac{1}{2}\epsilon_K) \quad (3.22)$$

for  $S(\Sigma_Q^{(*)}) \rightarrow T(\Lambda_Q)\pi$  and

$$Z'_1(5(a)) = 1 + \frac{9}{2}g_1^2(\frac{1}{8}\epsilon_\pi + \epsilon_K + \frac{1}{8}\epsilon_\eta) + 3g_2^2(-\frac{1}{4}\epsilon_\pi + \epsilon_K + \frac{3}{4}\epsilon_\eta) \quad (3.23)$$

for  $S(\Xi_Q^{(*)}) \rightarrow T(\Xi_Q)\pi$ .

The cancellation between the wave-function renormalization of the Goldstone bosons and the five-point vertex diagram for heavy meson strong decays also persists in the baryon sector. This can be understood from the fact that the five-point vertex in both cases arises from expanding the chiral field  $\mathcal{A}_\mu$  to the third power in  $M$  and hence has the same structure. Therefore  $Z_1(4(d)) = Z'_1(5(d)) = \sqrt{Z_2(\pi^a)}$ . Just like their counterparts in the meson sector, all the seagull diagrams in Figs. 4 and 5 also do not contribute to the strong decays  $S \rightarrow S\pi$  and  $S \rightarrow T\pi$  to the lowest order in heavy quark expansion. We thus conclude that

$$(g_1)_{\text{eff}} = g_1 \frac{Z_2(S)}{Z_1(4(a))} \quad (3.24)$$

and

$$(g_2)_{\text{eff}} = g_2 \frac{\sqrt{Z_2(S)Z_2(T)}}{Z'_1(5(a))}. \quad (3.25)$$

We now switch to the electromagnetic ( $M1$ ) decays  $S \rightarrow S + \gamma$  and  $S \rightarrow T + \gamma$ . The most general gauge-invariant Lagrangian for magnetic transitions of heavy baryons given in paper II [Eq. II.3.9] can be recast in terms of superfields<sup>6</sup>

$$\begin{aligned} \mathcal{L}_B^{(2)} = & -i3a_1 \text{tr}(\bar{S}^\mu Q F_{\mu\nu} S^\nu) \\ & + \sqrt{3}a_3 \epsilon_{\mu\nu\alpha\beta} \text{tr}(\bar{S}^\mu Q v^\nu F^{\alpha\beta} T) + \text{H. c.} \\ & + 3a'_1 \text{tr}(\bar{S}^\mu Q' \sigma \cdot F S_\mu) - \frac{3}{2}a'_1 \text{tr}(\bar{T} Q' \sigma \cdot FT), \end{aligned} \quad (3.26)$$

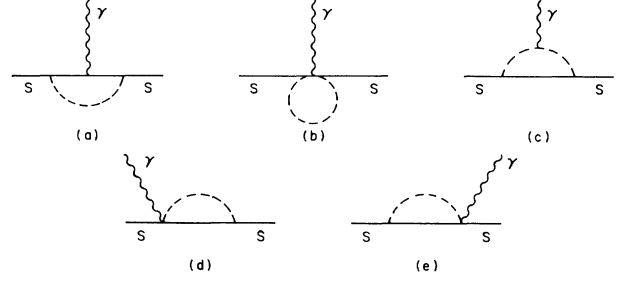


FIG. 7. Chiral-loop diagrams contributing to the radiative decay  $S \rightarrow T\gamma$ . In (a), the photon may originate from an  $SS\gamma$  or  $ST\gamma$  vertex with a coupling constant  $a_1$  or  $a_2$ . In (c), (d), and (e), the intermediate state is an  $S$  baryon.

where  $\sigma \cdot F \equiv \sigma_{\mu\nu} F^{\mu\nu}$  and we have applied Eqs. (II.3.47) and (II.3.61). The Lagrangian  $\mathcal{L}_B^{(2)}$  is also the most general chiral-invariant one, provided that one makes the replacement

$$Q \rightarrow \frac{1}{2}(\xi^\dagger Q \xi + \xi Q \xi^\dagger), \quad Q' \rightarrow Q'. \quad (3.27)$$

Note that contrary to Eq. (II.3.9), the Dirac magnetic moment terms do not appear in (3.26) because the Lagrangian  $\mathcal{L}_B^{(1)}$  is expressed in terms of velocity-dependent fields and hence does not contain Dirac magnetic moments to the lowest order. In the quark model, the magnetic moments  $a_1$  and  $a_2$  are simply related to the Dirac magnetic moments of the light quarks, whereas  $a'_1$  is connected to those of heavy quarks. Explicitly,  $a'_1$  is fixed by heavy quark symmetry to be  $\frac{1}{6}(e/2m_Q)$  and this is the only  $1/m_Q$  effect included for heavy baryon decays. In contrast, the couplings  $a_1$  and  $a_2$  are independent of the heavy quark mass and spin.

It follows from (3.26) that the tree amplitudes of heavy baryon radiative decays are given by

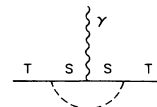


FIG. 8. Chiral-loop diagram contributing to the radiative decay  $T \rightarrow T\gamma$ . This is the only loop diagram contributing to the  $M1$  transition  $T \rightarrow T\gamma$ . All other possible diagrams do not contribute; see the footnote after Eq. (3.35) for discussion.

<sup>6</sup>The sign of the last two terms in Eq. (3.26) is opposite to those of the corresponding terms in Eq. (18) of Ref. [7].

$$A[S_{ij}^\mu(v) \rightarrow S_{ij}^\nu + \gamma(\varepsilon, k)] = i\frac{3}{2}a_1 \bar{U}^\nu(Q_{ii} + Q_{jj})(k_\nu \varepsilon_\mu - k_\mu \varepsilon_\nu) \mathcal{U}^\mu - i6a_1' Q' \bar{U}^\mu \mathcal{K} \mathcal{U}_\mu, \quad (3.28)$$

$$A[S_{ij}^\mu(v) \rightarrow T_{ij} + \gamma(\varepsilon, k)] = -2(\frac{3}{2})^{1/2} a_2 \varepsilon_{\mu\nu\alpha\beta} \bar{u}_3 v^\nu k^\alpha \varepsilon^\beta (Q_{ii} - Q_{jj}) \mathcal{U}^\mu \quad (i < j).$$

For the radiative decay  $S \rightarrow T + \gamma$ , the two light quarks in the heavy hadron must undergo a spin-flip transition. Consequently, such decays will not receive any contributions from the magnetic moment of the heavy quark. As we will see later, this property persists at the one-loop level. To the lowest order, we have the following predictions from (3.28):

$$\begin{aligned} A(\Xi_Q'^{1/2} \rightarrow \Xi_Q^{1/2} \gamma) &= A(\Sigma_Q^0 \rightarrow \Lambda_Q \gamma) = -\sqrt{2} a_2 \bar{u} \sigma_{\mu\nu} k^\mu \varepsilon^\nu u, \\ A(\Xi_Q'^{-1/2} \rightarrow \Xi_Q^{-1/2} \gamma) &= A(\Xi_Q'^{* -1/2} \rightarrow \Xi_Q^{-1/2} \gamma) = 0, \\ A(\Xi_Q'^{1/2} \rightarrow \Xi_Q^{1/2} \gamma) &= A(\Sigma_Q^{*0} \rightarrow \Lambda_Q \gamma) = -i\sqrt{6} a_2 \bar{u} (k_\mu \not{\varepsilon} - \varepsilon_\mu \not{k}) \gamma_5 u^\mu, \\ A(\Xi_Q'^{-1/2} \rightarrow \Xi_Q^{-1/2} \gamma) &= A(\Sigma_Q^{*-1} \rightarrow \Sigma_Q^{-1} \gamma) = A(\Omega_Q^* \rightarrow \Omega_Q \gamma) \\ &= -\frac{i}{\sqrt{3}} (a_1 - 8a_1') \bar{u} (k_\mu \not{\varepsilon} - \varepsilon_\mu \not{k}) \gamma_5 u^\mu, \\ A(\Xi_Q'^{1/2} \rightarrow \Xi_Q^{1/2} \gamma) &= A(\Sigma_Q^{*0} \rightarrow \Sigma_Q^0 \gamma) = \frac{i}{2\sqrt{3}} (a_1 + 16a_1') \bar{u} (k_\mu \not{\varepsilon} - \varepsilon_\mu \not{k}) \gamma_5 u^\mu, \end{aligned} \quad (3.29)$$

where the superscript denotes the isospin quantum number. The above SU(3) relations will be violated in the presence of chiral-loop contributions as depicted in Figs. 6 and 7. Chiral corrections will modify the coupling constants  $a_1$ ,  $a_1'$ , and  $a_2$  to

$$\begin{aligned} (a_1)_{\text{eff}} &= a_1 \frac{Z_2(S)}{Z_1} + \delta a_1 (6(c) + 6(d) + 6(e)), \\ (a_1')_{\text{eff}}(S) &= a_1' \frac{Z_2(S)}{Z_1'(SS\gamma)} = a_1', \\ (a_1')_{\text{eff}}(T) &= a_1' \frac{Z_2(T)}{Z_1'(TT\gamma)} = a_1', \\ (a_2)_{\text{eff}} &= a_2 \frac{\sqrt{Z_2(S)Z_2(T)}}{Z_1''} + \delta a_2 (7(c) + 7(d) + 7(e)), \end{aligned} \quad (3.30)$$

where  $Z_1$  [ $Z_1'(SS\gamma)$ ],  $Z_1''$ , and  $Z_1'(TT\gamma)$  are the vertex renormalization constants induced by Figs. 6(a), 6(b), 7(a), 7(b), and 8, respectively. In (3.30) we have anticipated the results [see (3.33) and (3.35) below]  $Z_2(S) = Z_1'(SS\gamma)$  and  $Z_2(T) = Z_1'(TT\gamma)$ . We remark that since  $\Xi_Q'^{-1/2(*)} \rightarrow \Xi_Q^{-1/2} \gamma$  is prohibited at the tree level, its effective coupling  $(a_2)_{\text{eff}}$  is defined in a similar way as  $\Xi_Q'^{1/2(*)} \rightarrow \Xi_Q^{1/2} \gamma$ :

$$A[S(\Xi_Q'^{-1/2(*)}) \rightarrow T(\Xi_Q^{-1/2}) \gamma] = -2(\frac{3}{2})^{1/2} (a_2)_{\text{eff}} \bar{u} \varepsilon_{\mu\nu\alpha\beta} v^\nu k^\alpha \varepsilon^\beta \mathcal{U}^\mu, \quad (3.31)$$

with

$$(a_2)_{\text{eff}} = \delta a_2 (7(a) + 7(b) + 7(c) + 7(d) + 7(e)). \quad (3.32)$$

Having calculated the renormalization constants  $Z_2(S)$  and  $Z_2(T)$  earlier, we now proceed to evaluate Figs. 6(a), 6(b), 7(a), 7(b), and 8 for the vertex renormalization constants  $Z_1$ ,  $Z_1'$ , and  $Z_1''$ . Note that charge couplings for the vertices  $SS\gamma$  and  $TT\gamma$  in Fig. 6(a) and  $SS\gamma$  in Fig. 7(a) are proportional to  $(v \cdot \varepsilon)$  and consequently cannot induce magnetic transitions. The contributions to  $Z_1$  due to the magnetic  $SS\gamma$  and  $ST\gamma$  couplings can be summarized as follows:

$$Z_1(SS\gamma; 6(a)) = 1 + \sum_b \left[ \frac{9}{4} g_1^2 \tilde{\xi}_{ij} - 6 \frac{a_2}{a_1} g_1 g_2 \bar{\xi}_{ij} \right] \frac{\varepsilon_{\pi^b}}{Q_{ii} + Q_{jj}}, \quad (3.33a)$$

$$Z_1'(SS\gamma; 6(a)) = Z_2(S), \quad (3.33b)$$

with

$$\begin{aligned} \tilde{\xi}_{ij} &= \frac{1}{8} \{ (\lambda^b Q \lambda^b)_{jj} + (\lambda^b \lambda^b)_{jj} Q_{ii} + 2\lambda_{ji}^b \lambda_{ij}^b Q_{ii} + \lambda_{jj}^b \lambda_{ii}^b (Q_{ii} + Q_{jj}) (1 - \delta_{ij}) + (i \leftrightarrow j) \}, \\ \bar{\xi}_{ij} &= \frac{1}{4} \{ (\lambda^b Q \lambda^b)_{jj} - (\lambda^b \lambda^b)_{jj} Q_{ii} + (i \leftrightarrow j) \} \end{aligned} \quad (3.34)$$

for  $S_{ij} \rightarrow S_{ij} + \gamma$ ,

$$Z_1'(TT\gamma; 8) = Z_2(T) \quad (3.35)$$

for<sup>7</sup>  $T_{ij} \rightarrow T_{ij} + \gamma$ , and

$$Z_1''(ST\gamma; 7(a)) = 1 + \sum_b \left[ -\frac{9\sqrt{2}}{4} g_1 g_2 \frac{a_1}{a_2} \frac{\tilde{\xi}_{ij}''}{Q_{ii} - Q_{jj}} + \frac{3}{\sqrt{2}} g_2^2 \frac{\tilde{\xi}_{ij}''}{Q_{ii} - Q_{jj}} \right] \epsilon_{\pi^b} \quad (i < j), \quad (3.36)$$

with

$$\begin{aligned} \tilde{\xi}_{ij}'' &= \frac{1}{4\sqrt{2}} [(\lambda^b Q \lambda^b)_{ii} + (\lambda^b \lambda^b)_{ii} Q_{jj} + 2\lambda_{ij}^b \lambda_{ji}^b Q_{jj} - (i \leftrightarrow j)], \\ \tilde{\xi}_{ij}'' &= \frac{1}{2\sqrt{2}} [(\lambda^b Q \lambda^b)_{ii} - (\lambda^b \lambda^b)_{ii} Q_{jj} + \lambda_{ii}^b \lambda_{jj}^b (Q_{jj} - Q_{ii}) - (i \leftrightarrow j)] \end{aligned} \quad (3.37)$$

for  $S_{ij} \rightarrow T_{ij} + \gamma$ . Equations (3.33b) and (3.35) imply that the parameter  $a_1'$  in (3.30) is not renormalized. This confirms an exact QCD result that  $a_1'$  does not get renormalized [13] in chiral perturbation theory. Note that when  $Q_{ii} = Q_{jj}$ , the tree amplitude for  $S \rightarrow T + \gamma$  vanishes [see Eq. (3.28)] and  $Z_1'$  is undefined. In this case, one should apply Eqs. (3.31) and (3.32). The explicit expressions of the vertex renormalization constant  $Z_1$  for each radiative decay mode are then given by

$$\begin{aligned} Z_1(\Sigma_Q^{+1(*)} \rightarrow \Sigma_Q^+ \gamma; 6(a)) &= 1 + \frac{9}{8} g_1^2 (\frac{5}{4} \epsilon_\pi + \frac{1}{4} \epsilon_K + \frac{1}{3} \epsilon_\eta) + \frac{9}{2} g_1 g_2 \frac{a_2}{a_1} (\epsilon_\pi + \epsilon_K), \\ Z_1(\Sigma_Q^{0(*)} \rightarrow \Sigma_Q^0 \gamma; 6(a)) &= 1 + \frac{9}{4} g_1^2 (\epsilon_\pi - \frac{1}{4} \epsilon_K + \frac{1}{6} \epsilon_\eta) + 9 g_1 g_2 \frac{a_2}{a_1} (\epsilon_K), \\ Z_1(\Sigma_Q^{-1(*)} \rightarrow \Sigma_Q^- \gamma; 6(a)) &= 1 + \frac{9}{8} g_1^2 (\frac{1}{2} \epsilon_\pi + \epsilon_K + \frac{1}{3} \epsilon_\eta) + 9 g_1 g_2 \frac{a_2}{a_1} (\epsilon_\pi), \\ Z_1(\Xi_Q'^{1/2(*)} \rightarrow \Xi_Q'^{1/2} \gamma; 6(a)) &= 1 + \frac{27}{16} g_1^2 (-\frac{1}{2} \epsilon_\pi + \frac{5}{3} \epsilon_K + \frac{1}{18} \epsilon_\eta) + \frac{9}{2} g_1 g_2 \frac{a_2}{a_1} (-\epsilon_\pi + 2\epsilon_K + \epsilon_\eta), \\ Z_1(\Xi_Q'^{-1/2(*)} \rightarrow \Xi_Q'^{-1/2} \gamma; 6(a)) &= 1 + \frac{9}{32} g_1^2 (7\epsilon_K + \frac{1}{3} \epsilon_\eta) + \frac{9}{2} g_1 g_2 \frac{a_2}{a_1} (\epsilon_\pi + \epsilon_K), \\ Z_1(\Omega_Q^{(*)} \rightarrow \Omega_Q \gamma; 6(a)) &= 1 + \frac{3}{4} g_1^2 (\frac{3}{4} \epsilon_K + 2\epsilon_\eta) + 9 g_1 g_2 \frac{a_2}{a_1} (\epsilon_K), \end{aligned} \quad (3.38)$$

and

$$\begin{aligned} Z_1''(\Sigma_Q^{0(*)} \rightarrow \Lambda_Q \gamma; 7(a)) &= 1 + \frac{9}{2} g_1 g_2 \frac{a_1}{a_2} (\epsilon_\pi + \frac{1}{4} \epsilon_K) + 3 g_2^2 (\epsilon_\pi + \frac{1}{2} \epsilon_K), \\ Z_1''(\Xi_Q'^{1/2(*)} \rightarrow \Xi_Q'^{1/2} \gamma; 7(a)) &= 1 + \frac{9}{8} g_1 g_2 \frac{a_1}{a_2} (\frac{1}{2} \epsilon_\pi + \frac{13}{3} \epsilon_K + \frac{1}{6} \epsilon_\eta) + \frac{3}{4} g_2^2 (\epsilon_\pi + 2\epsilon_K + 3\epsilon_\eta), \\ \delta a_2(\Xi_Q'^{-1/2(*)} \rightarrow \Xi_Q'^{-1/2} \gamma; 7(a)) &= \frac{3}{8} g_1 g_2 a_1 (-\epsilon_K + \epsilon_\eta) + \frac{3}{2} g_2^2 a_2 (-\epsilon_\pi + \epsilon_K), \end{aligned} \quad (3.39)$$

for  $S \rightarrow T + \gamma$ . Recall that the heavy quark magnetic moment  $a_1'$  does not contribute to the  $S \rightarrow T\gamma$  transitions at the tree level. Here we see that this consequence of the heavy quark symmetry is preserved at the loop level.

The electromagnetic five-point vertices in Figs. 6(b) and 7(b) are generated by the Lagrangian (3.26) with the replacement  $Q \rightarrow (1/4f_0^2)[M, [Q, M]]$ , which comes from (3.27). The results are

$$\begin{aligned} Z_1(S_{ij} \rightarrow S_{ij} + \gamma; 6(b)) &= 1 + \frac{1}{4} \sum_b \{ [\lambda^b, [Q, \lambda^b]]_{ii} + (i \rightarrow j) \} \frac{\epsilon_{\pi^b}}{Q_{ii} + Q_{jj}}, \\ Z_1''(S_{ij} \rightarrow T_{ij} + \gamma; 7(b)) &= 1 + \frac{1}{4} \sum_b \{ [\lambda^b, [Q, \lambda^b]]_{ii} - (i \rightarrow j) \} \frac{\epsilon_{\pi^b}}{Q_{ii} - Q_{jj}} \quad (i < j). \end{aligned} \quad (3.40)$$

<sup>7</sup>Since the magnetic  $TT\gamma$  coupling vanishes in heavy quark limit and chiral corrections preserve heavy quark symmetry, we can be sure that no other diagrams such as the seagull diagrams and the diagram such as Fig. 8 but with a photon attached to the light meson can contribute to  $Z_1(T \rightarrow T\gamma)$ . We have checked this explicitly.

Explicit expressions for  $Z_1(6(b))$  and  $Z_1''(7(b))$  for individual decay modes read

$$\begin{aligned} Z_1(\Sigma_Q^{+1(*)} \rightarrow \Sigma_Q^+ \gamma; 6(b)) &= Z_1(\Xi_Q'^{-1/2(*)} \rightarrow \Xi_Q'^{-1/2} \gamma; 6(b)) = 1 - \frac{3}{2}(\epsilon_\pi + \epsilon_K) , \\ Z_1(\Omega_Q^{(*)} \rightarrow \Omega_Q \gamma; 6(b)) &= Z_1(\Sigma_Q^{0(*)} \rightarrow \Sigma_Q^0 \gamma; 6(b)) = 1 - 3\epsilon_K , \\ Z_1(\Sigma_Q^{-1(*)} \rightarrow \Sigma_Q^- \gamma; 6(b)) &= Z_1(\Xi_Q'^{1/2(*)} \rightarrow \Xi_Q'^{1/2} \gamma; 6(b)) = 1 - 3\epsilon_\pi , \end{aligned} \quad (3.41)$$

and

$$\begin{aligned} Z_1''(\Sigma_Q^{0(*)} \rightarrow \Lambda_Q \gamma; 7(b)) &= 1 - (2\epsilon_\pi + \epsilon_K) , \\ Z_1''(\Xi_Q'^{1/2(*)} \rightarrow \Xi_Q'^{1/2} \gamma; 7(b)) &= 1 - (\epsilon_\pi + 2\epsilon_K) , \\ \delta a_2(\Xi_Q'^{-1/2(*)} \rightarrow \Xi_Q'^{-1/2} \gamma; 7(b)) &= (-\epsilon_\pi + \epsilon_K) a_2 . \end{aligned} \quad (3.42)$$

Figures 6(c) and 7(c) are the Feynman diagrams in which a photon couples to light pseudoscalar mesons. By applying Eqs. (A3) and (A5), we arrive at

$$A_\pi(S; 6(c)) = i \frac{9}{256} \frac{m_\pi}{\pi} \frac{g_1^2}{f_0^2} \bar{u}^\nu(k_\nu \epsilon_\mu - k_\mu \epsilon_\nu) \mathcal{U}^\mu . \quad (3.43)$$

Likewise, the amplitude for the charged pion loop with antitriplet baryon intermediate state reads

$$A_\pi(T; 6(c)) = i \frac{3}{32} \frac{m_\pi}{\pi} \frac{g_2^2}{f_0^2} \bar{u}^\nu(k_\nu \epsilon_\mu - k_\mu \epsilon_\nu) \mathcal{U}^\mu . \quad (3.44)$$

Therefore the radiative decay amplitude due to the sextet or antitriplet intermediate baryon state is separately gauge invariant, as it should be. Projecting out the spin- $\frac{1}{2}$  final state from Eqs. (3.43) and (3.44) gives

$$A_\pi(\Sigma_Q^{*+1} \rightarrow \Sigma_Q^+ \gamma; 6(c)) = i \frac{\sqrt{3}}{32} \frac{m_\pi}{\pi f_0^2} \left[ \frac{3}{8} g_1^2 + g_2^2 \right] \bar{u}(k_\mu \not{\epsilon} - \epsilon_\mu \not{k}) \gamma_5 u^\mu . \quad (3.45)$$

Comparing this with the tree amplitude

$$A(\Sigma_Q^{*+1} \rightarrow \Sigma_Q^+ \gamma)_{\text{tree}} = i \frac{2}{\sqrt{3}} (a_1 + 6a_1' e_Q) \bar{u}(k_\mu \not{\epsilon} - \epsilon_\mu \not{k}) \gamma_5 u^\mu \quad (3.46)$$

leads to

$$\delta a_1(\Sigma_Q^{*+1} \rightarrow \Sigma_Q^+ \gamma; 6(c)) = \frac{3e}{64\pi} \left[ \frac{3}{8} g_1^2 + g_2^2 \right] \frac{m_\pi}{f_0^2} \quad (3.47)$$

for charged pion loops. The general results including all charged meson loops are [see Appendix B for a derivation of the SU(3) group factors]

$$\begin{aligned} \delta a_1(6(c)) &= \sum_b \frac{e}{32\pi} \frac{m_{\pi^b}}{f_0^2} \left[ \frac{3}{4} g_1^2 \bar{\xi}_{ij} + g_2^2 \bar{\xi}'_{ij} \right] \frac{1}{Q_{ii} + Q_{jj}} , \\ \delta a_2(7(c)) &= \sum_b \frac{3e}{64\sqrt{2}\pi} g_1 g_2 \frac{m_{\pi^b}}{f_0^2} \frac{\bar{\xi}'_{ij}}{Q_{ii} - Q_{jj}} \quad (i < j) , \end{aligned} \quad (3.48)$$

with

$$\begin{aligned} \bar{\xi}_{ij} &= -\frac{1}{4} \{([\lambda^b, Q] \lambda^b)_{ii} + (i \leftrightarrow j)\} , \\ \bar{\xi}_{ij} &= -\frac{1}{2} \{([\lambda^b, Q] \lambda^b)_{ii} + (i \leftrightarrow j)\} , \\ \bar{\xi}'_{ij} &= -\frac{1}{2\sqrt{2}} \{([\lambda^b, Q] \lambda^b)_{ii} + [\lambda^b, Q]_{ij} \lambda_{ji}^b - (i \leftrightarrow j)\} . \end{aligned} \quad (3.49)$$

Working out the above general expressions we obtain

$$\begin{aligned}
\delta a_1(\Sigma_Q^{+1(*)} \rightarrow \Sigma_Q^{+1}\gamma; 6(c)) &= \delta a_1(\Xi_Q'^{-1/2(*)} \rightarrow \Xi_Q'^{-1/2}\gamma; 6(c)) = \frac{3e}{64\pi} \left[ \frac{3}{8}g_1^2 + g_2^2 \right] \left[ \frac{m_\pi}{f_0^2} + \frac{m_K}{f_0^2} \right], \\
\delta a_1(\Omega_Q^{(*)} \rightarrow \Omega_Q\gamma; 6(c)) &= \delta a_1(\Sigma_Q^{0(*)} \rightarrow \Sigma_Q^0\gamma; 6(c)) = \frac{3e}{32\pi} \left[ \frac{3}{8}g_1^2 + g_2^2 \right] \left[ \frac{m_K}{f_0^2} \right], \\
\delta a_1(\Sigma_Q^{-1(*)} \rightarrow \Sigma_Q^{-1}\gamma; 6(c)) &= \delta a_1(\Xi_Q'^{1/2(*)} \rightarrow \Xi_Q'^{1/2}\gamma; 6(c)) = \frac{3e}{32\pi} \left[ \frac{3}{8}g_1^2 + g_2^2 \right] \left[ \frac{m_\pi}{f_0^2} \right]
\end{aligned} \tag{3.50}$$

and

$$\begin{aligned}
\delta a_2(\Sigma_Q^{0(*)} \rightarrow \Lambda_Q\gamma; 7(c)) &= \frac{3e}{32} \frac{g_1 g_2}{\pi} \left[ \frac{m_\pi}{f_0^2} + \frac{1}{4} \frac{m_K}{f_0^2} \right], \\
\delta a_2(\Xi_Q'^{1/2(*)} \rightarrow \Xi_Q'^{1/2}\gamma; 7(c)) &= \frac{3e}{32} \frac{g_1 g_2}{\pi} \left[ \frac{1}{4} \frac{m_\pi}{f_0^2} + \frac{m_K}{f_0^2} \right], \\
\delta a_2(\Xi_Q'^{-1/2(*)} \rightarrow \Xi_Q'^{-1/2}\gamma; 7(c)) &= \frac{3e}{128} \frac{g_1 g_2}{\pi} \left[ -\frac{m_\pi}{f_0^2} + \frac{m_K}{f_0^2} \right].
\end{aligned} \tag{3.51}$$

Note that  $\delta a_2$  for the decay  $\Xi_Q'^{-1/2(*)} \rightarrow \Xi_Q'^{-1/2}$  is defined in Eqs. (3.31) and (3.32) and it does not contain the factor of  $1/(Q_{ii} - Q_{jj})$ . In the SU(3) limit, all the above results (3.38)–(3.51) do satisfy the SU(3) relations given by (3.29).

As in the meson case, the seagull diagrams depicted in Figs. 6(d), 6(e), 7(d), and 7(e) do not contribute. The arguments are similar to those given in Sec. II and will not be repeated here. Hence

$$\delta a_1(6(d) + 6(e)) = \delta a_2(7(d) + 7(e)) = 0. \tag{3.52}$$

Finally, we note that the vertices  $SS\pi^a$  and  $ST\pi^a$  in the Lagrangian (3.4) may suggest that there is a possibility of mixing between the sextet and antitriplet baryons through loop effects. However, this is not the case. An explicit calculation shows that such loop diagrams vanish. The only possible mixing between  $S$  and  $T$  requires an  $\epsilon_{\mu\nu\alpha\beta}$  tensor, but there are not enough variables to construct a Lorentz invariant.

In summary, taking into account the mass differences among the Goldstone bosons, we found that SU(3) relations are generally broken in the strong and radiative decays of heavy hadrons. The leading chiral-loop corrections have nonanalytic dependence on  $m_q$  of the form  $m_q^{1/2}$  or  $m_q \ln m_q$ .

#### IV. APPLICATIONS

In Secs. II and III we have presented a general analysis of SU(3)-breaking effects in chiral perturbation theory for the strong and  $M1$  radiative decays of heavy mesons and heavy baryons. In this section we will apply the results obtained so far to some selected decay modes of charmed mesons and baryons. Specifically, we choose the radiative decays  $D^* \rightarrow D\gamma$ ,  $\Sigma_c \rightarrow \Lambda_c\gamma$ ,  $\Xi_c' \rightarrow \Xi_c\gamma$ ,  $\Xi_c'^* \rightarrow \Xi_c'\gamma$ ,  $\Sigma_c^* \rightarrow \Sigma_c\gamma$ ,  $\Omega_c^* \rightarrow \Omega_c\gamma$  and the strong decays  $D^* \rightarrow D\pi$ ,  $\Sigma_c \rightarrow \Lambda_c\pi$  as examples of applications. The decay rates of many of these modes have been explicitly calculated in papers I and II. Special attention is paid to the SU(3) re-

lations (2.41) and (3.29) for radiative decays. There are nonanalytic  $m_q^{1/2}$  and  $m_q \ln m_q$  chiral corrections which are responsible for SU(3) violation in chiral perturbation theory. In paper II, the relevant couplings are obtained from the quark model and they are related to the constituent quark masses. Hence SU(3) violation is already incorporated there. In this section, a comparison between the two different approaches for SU(3) violation is made.

We begin with the  $D^* \rightarrow D\pi$  decay. When chiral-loop corrections are included, we recall from Sec. II that its decay amplitude is given by<sup>8</sup>

$$A(D_i^* \rightarrow D_j\pi^a) = \frac{g_{\text{eff}}}{f_0} \sqrt{M_D M_{D^*}} (\lambda^a)_{ij} (\epsilon^* \cdot q), \tag{4.1}$$

where  $g_{\text{eff}}$  has been defined in Eq. (2.28) and  $q$  is the pion momentum. The decay widths implied by the amplitude (4.1) are

$$\begin{aligned}
\Gamma(D^* \rightarrow D\pi^+) &= \frac{1}{12\pi} \left[ \frac{g_{\text{eff}}}{f_0} \right]^2 \frac{M_D M_{D^*}}{(M_{D^*}^{\text{phys}})^2} q^3, \\
\Gamma(D^* \rightarrow D\pi^0) &= \frac{1}{24\pi} \left[ \frac{g_{\text{eff}}}{f_0} \right]^2 \frac{M_D M_{D^*}}{(M_{D^*}^{\text{phys}})^2} q^3.
\end{aligned} \tag{4.2}$$

Note that  $D_s^{*+} \rightarrow D_s^+\pi^0$  is prohibited by isospin symmetry and  $D^{*0} \rightarrow D^+\pi^-$  is kinematically forbidden. The unrenormalized masses  $M_P$  and  $M_{P^*}$  appearing in (2.1), (2.2), (4.1), and (4.2) can be inferred from the experimental measurement of heavy meson mass differences. First,

<sup>8</sup>Chiral logarithmic corrections to the decay  $D^{*+} \rightarrow D^0\pi^+$  are also calculated in Ref. [19] with the up and down quark masses being neglected. We agree with the results of Ref. [19] if the same approximation is made.

the SU(3)-invariant  $\alpha_3$  term in Eq. (2.18) can be absorbed into a redefinition of  $M_p$  and  $M_{p^*}$ . Then (2.16) and (2.18) yield

$$\begin{aligned} M_{D^+}^{\text{phys}} - M_D &= M_{D^{*+}}^{\text{phys}} - M_{D^*} \\ &= -\alpha_1 m_d - \frac{g^2}{32\pi} \left[ 3 \frac{m_\pi^3}{f_0^2} + 2 \frac{m_K^3}{f_0^2} + \frac{1}{3} \frac{m_\eta^3}{f_0^2} \right] \end{aligned} \quad (4.3a)$$

and

$$\begin{aligned} M_{D_s^+}^{\text{phys}} - M_D &= M_{D_s^{*+}}^{\text{phys}} - M_{D^*} \\ &= -\alpha_1 m_s - \frac{g^2}{32\pi} \left[ 4 \frac{m_K^3}{f_0^2} + \frac{4}{3} \frac{m_\eta^3}{f_0^2} \right]. \end{aligned} \quad (4.3b)$$

Equation (4.3) implies the mass difference<sup>9</sup>

$$\begin{aligned} M_{D_s^+}^{\text{phys}} - M_{D^+}^{\text{phys}} &= M_{D_s^{*+}}^{\text{phys}} - M_{D^{*+}}^{\text{phys}} \\ &= -\alpha_1 (m_s - m_d) \\ &\quad - \frac{g^2}{32\pi} \left[ -3 \frac{m_\pi^3}{f_0^2} + 2 \frac{m_K^3}{f_0^2} + \frac{m_\eta^3}{f_0^2} \right]. \end{aligned} \quad (4.4)$$

Note that formula (4.4) is different from that of Ref. [20] by a factor of  $\frac{4}{3}$  for the second term on the RHS. The parameter  $\alpha_1$  can be determined from the measured value  $M_{D_s^+}^{\text{phys}} - M_{D^+}^{\text{phys}} = 99.5 \pm 0.6$  MeV [21], the current quark masses  $m_s = 199$  MeV,  $m_d = 9.9$  MeV [22], and the value of  $g$  chosen. The unrenormalized masses  $M_D$  and  $M_{D^*}$  can then be solved from (4.3).<sup>10</sup>

We digress here to comment on the quantity

$$\begin{aligned} \Delta_D &\equiv (M_{D_s^+}^{\text{phys}} - M_{D^+}^{\text{phys}}) - (M_{D_s^{*+}}^{\text{phys}} - M_{D^{*+}}^{\text{phys}}) \\ &= (M_{D_s^{*+}}^{\text{phys}} - M_{D^+}^{\text{phys}}) - (M_{D_s^{*+}}^{\text{phys}} - M_{D^{*+}}^{\text{phys}}), \end{aligned} \quad (4.5)$$

with the experimental value [21,23]

$$\Delta_D = (0.9 \pm 1.9) \text{ MeV}, \quad (4.6)$$

<sup>9</sup>In the presence of  $1/m_Q$  corrections, the heavy quark symmetry relations  $\alpha_2 = -\alpha_1$  and  $g = f/2$  are no longer valid and Eq. (4.4) is modified to

$$\begin{aligned} M_{D_s^+}^{\text{phys}} - M_{D^+}^{\text{phys}} &= -\alpha_1 (m_s - m_d) \\ &\quad - \frac{f^2}{128\pi} \left[ -3 \frac{m_\pi^3}{f_0^2} + 2 \frac{m_K^3}{f_0^2} + \frac{m_\eta^3}{f_0^2} \right], \\ M_{D_s^{*+}}^{\text{phys}} - M_{D^{*+}}^{\text{phys}} &= \alpha_2 (m_s - m_d) \\ &\quad - \frac{1}{128\pi} \left[ \frac{8}{3} g^2 + \frac{1}{3} f^2 \right] \\ &\quad \times \left[ -3 \frac{m_\pi^3}{f_0^2} + 2 \frac{m_K^3}{f_0^2} + \frac{m_\eta^3}{f_0^2} \right]. \end{aligned}$$

<sup>10</sup>At the preferred value  $g = 0.52$  as shown below, we obtain  $M_D = 1971$  MeV and  $M_{D^*} = 2112$  MeV.

which has recently received a lot of attention [24]. Obviously,  $\Delta_D$  vanishes in either the heavy quark or chiral limit. Beyond these limits,  $\Delta_D$  received two types of contributions. The first type is from the tree contribution induced by the  $1/m_c$  corrections to the relation  $\alpha_1 = -\alpha_2$ . The second type comes from the self-energy one-loop diagrams with an insertion of lowest-order mass splitting  $\Delta M^2 P(v) P^\dagger(v)$  and the ones without the above insertion but taking into account the splitting of  $g$  and  $f/2$ . This was discussed in detail in our earlier paper [13] on heavy quark symmetry-breaking effects.

For the radiative decays  $D^* \rightarrow D\gamma$ , we see from Eq. (2.51) that the leading chiral corrections are dominated by Fig. 2(e) and the wave-function and vertex renormalizations. Before making concrete estimates on the parameter  $\rho_i$  [cf. Eq. (2.37)], recall that in paper II we have considered the constituent quark model and incorporated SU(3) breaking into the light quark charge matrix

$$Q \rightarrow \tilde{Q} = \begin{pmatrix} \frac{2}{3} & 0 & 0 \\ 0 & -\frac{1}{3} \frac{M_u}{M_d} & 0 \\ 0 & 0 & -\frac{1}{3} \frac{M_u}{M_s} \end{pmatrix}. \quad (4.7)$$

To avoid any confusion with the current quark mass  $m_q$ , we have used capital letters to denote the constituent quark mass in (4.7). Therefore the ‘‘effective’’ parameters  $(\beta_{\text{eff}})_i$  are identical to  $1/M_u$ ,  $1/M_d$ , and  $1/M_s$ , respectively, for  $D_i^* \rightarrow D_i + \gamma$  ( $i = 1, 2, 3$ ), and hence in the quark model

$$\rho_i^{\text{QM}} = e \sqrt{M_{D_i}^{\text{phys}} M_{D_i^*}^{\text{phys}}} \left[ \frac{e_i}{M_{q_i}} + \frac{2}{3} \frac{1}{m_c} \right]. \quad (4.8)$$

Using the constituent quark masses from the Particle Data Group [21],<sup>11</sup>

$$M_u = 338 \text{ MeV}, \quad M_d = 322 \text{ MeV}, \quad M_s = 510 \text{ MeV}, \quad (4.9)$$

we get

$$\rho_1^{\text{QM}} = 4.62e, \quad \rho_2^{\text{QM}} = -1.20e, \quad \rho_3^{\text{QM}} = -0.49e, \quad (4.10)$$

for  $m_c = 1.6$  GeV. The effective coupling  $\rho_i$  enters the radiative decay rate via

$$\Gamma(D_i^* \rightarrow D_i + \gamma) = \frac{\rho_i^2}{12\pi (M_{D_i^*}^{\text{phys}})^2} k^3, \quad (4.11)$$

with  $k$  being the photon momentum in the c.m. frame.

Recall that the quark model predictions agree very well with the two existing data on the  $D^*$  decays [10]: the upper limit on the total width of  $D^{*+}$  [12] and the branching ratio measurements by CLEO II [11]. It would be very important to see how well chiral perturbation theory does in this regard. There are four unknown

<sup>11</sup>These values of the constituent quark masses are given on p. VIII.59 of Ref. [21].

TABLE I. Predicted decay rates (in units of keV) and branching ratios (in parentheses) of strong and electromagnetic decays of charmed mesons for various values of  $g$  with  $\beta=2.6 \text{ GeV}^{-1}$  and  $m_c=1.6 \text{ GeV}$ . For comparison, the quark model predictions [10] and the experimental branching ratios measured by CLEO II [11] are given in the last two columns. The numbers under “quark model” differ somewhat from those given in Ref. [10] because of the more precise pion masses used here.

Reaction	$g=0.5$	$g=0.52$	$g=0.6$	$g=0.75$	Quark model	CLEO II
$D^{*+} \rightarrow D^0 \pi^+$	78.8 (68%)	87.9 (68%)	133.4 (68%)	276.0 (68%)	102 (68%)	$(68.1 \pm 1.0 \pm 1.3)\%$
$D^{*+} \rightarrow D^+ \pi^0$	35.7 (31%)	39.8 (31%)	60.5 (31%)	125.0 (31%)	46 (31%)	$(30.8 \pm 0.4 \pm 0.8)\%$
$D^{*+} \rightarrow D^+ \gamma$	1.9 (1.7%)	2.0 (1.5%)	2.1 (1.1%)	2.5 (0.6%)	2 (1.3%)	$(1.1 \pm 1.4 \pm 1.6)\%$
$D^{*+} \rightarrow \text{total}$	116.4	129.7	196.0	403.5	150	
$D^{*0} \rightarrow D^0 \pi^0$	54.1 (61%)	60.3 (65%)	91.5 (76%)	189.3 (90%)	70 (67%)	$(63.6 \pm 2.3 \pm 3.3)\%$
$D^{*0} \rightarrow D^0 \gamma$	34.0 (39%)	33.0 (35%)	28.9 (24%)	19.9 (10%)	34 (33%)	$(36.4 \pm 2.3 \pm 3.3)\%$
$D^{*0} \rightarrow \text{total}$	88.1	93.3	120.4	209.2	104	
$D_s^{*+} \rightarrow D_s^+ \gamma$	4.6	4.5	3.7	2.1	0.3	

TABLE II. Same as Table I except for  $\beta=3.0 \text{ GeV}^{-1}$ .

Reaction	$g=0.5$	$g=0.52$	$g=0.6$	$g=0.75$	Quark model	CLEO II
$D^{*+} \rightarrow D^0 \pi^+$	78.8 (67%)	87.9 (67%)	133.4 (67%)	276.0 (68%)	102 (68%)	$(68.1 \pm 1.0 \pm 1.3)\%$
$D^{*+} \rightarrow D^+ \pi^0$	35.7 (30%)	39.8 (30%)	60.5 (31%)	125.0 (31%)	46 (31%)	$(30.8 \pm 0.4 \pm 0.8)\%$
$D^{*+} \rightarrow D^+ \gamma$	3.4 (3%)	3.4 (3%)	3.8 (2%)	4.7 (1%)	2 (1.3%)	$(1.1 \pm 1.4 \pm 1.6)\%$
$D^{*+} \rightarrow \text{total}$	117.9	131.1	197.7	405.7	150	
$D^{*0} \rightarrow D^0 \pi^0$	54.1 (53%)	60.3 (56%)	91.5 (67%)	189.3 (85%)	70 (67%)	$(63.6 \pm 2.3 \pm 3.3)\%$
$D^{*0} \rightarrow D^0 \gamma$	47.5 (47%)	46.7 (44%)	42.6 (33%)	33.3 (15%)	34 (33%)	$(36.4 \pm 2.3 \pm 3.3)\%$
$D^{*0} \rightarrow \text{total}$	101.6	107.0	134.1	222.6	104	
$D_s^{*+} \rightarrow D_s^+ \gamma$	8.3	8.2	7.5	6.0	0.3	

parameters in the theory:  $g$ ,  $\beta$ ,  $m_c$ , and  $\Lambda$ , and available data do not permit an unambiguous determination of these parameters. Furthermore, other corrections such as  $1/m_Q$  effects may be of comparable importance as the chiral-loop corrections. Unfortunately, these  $1/m_Q$  corrections are difficult to estimate [13]. Consequently, we will take a modest approach. We will set  $m_c=1.6 \text{ GeV}$  and  $\Lambda=\Lambda_\chi \sim 1 \text{ GeV}$ , the chiral-symmetry-breaking scale. Then, for  $\beta=2.6 \text{ GeV}^{-1}$  and  $3.0 \text{ GeV}^{-1}$ , we let  $g$  take several different values at  $g=0.5, 0.52, 0.60$ , and  $0.75$ . The results are presented in Tables I and II.<sup>12</sup> We see that for the total width of  $D^{*+}$  to be of order 130 keV or less we must have  $g \lesssim 0.52$ . On the other hand, the branching ratios for the  $D^{*0}$  measured by CLEO II appear to favor  $g=0.52$  and  $\beta=2.6 \text{ GeV}^{-1}$ . For this particular choice of  $g$  and  $\beta$ , the predictions are quite close to the quark model results except for the radiative decay of  $D_s^{*+}$ . The decay rate for  $D_s^{*+} \rightarrow D_s^+ \gamma$  is larger by an order of magnitude in chiral perturbation theory than in the quark model. Specifically, we find from Eq. (2.51) that

$$\rho_1=4.59e, \quad \rho_2=-1.14e, \quad \rho_3=-1.79e, \quad (4.12)$$

which should be compared with the quark model prediction (4.10). Of course, there is no reason to expect that

these two different approaches for SU(3) violation should agree with each other exactly. Loosely speaking, SU(3) violation is treated nonperturbatively in the nonrelativistic quark model, while it is calculated in terms of a perturbative expansion in chiral effective Lagrangian theory. Nevertheless, the fact that the predicted decay rates and branching ratios for  $D^{*+}$  and  $D^{*0}$  agree so well with the quark model and the data suggests a consistency between “model and theory.” It will be extremely interesting to measure the rate for  $D_s^{*+} \rightarrow D_s^+ \gamma$  to see which prediction, if any, is closer to the truth. It is obvious from Table I that a smaller total width of the  $D^{*+}$  [12] can be easily accommodated without upsetting the agreement of the predicted branching ratios for both  $D^{*+}$  and  $D^{*0}$  with the CLEO II data [11].

At this point it is worthwhile to compare our favored choice of  $g=0.52$  and  $\beta=2.6 \text{ GeV}^{-1}$  in chiral perturbation theory with the corresponding parameters  $g_{\text{QM}}$  and  $\beta_{\text{QM}}$  in the quark model. Recall that  $g_{\text{QM}}=0.75$  [3] and  $\beta_{\text{QM}}=1/M_u=2.96 \text{ GeV}^{-1}$  [10]. Since  $g_{\text{QM}}$  is nonperturbative in nature while  $g$  is an unrenormalized parameter in the chiral Lagrangian approach, they are *a priori* not the same. To see their relation, we write down the  $D^* \rightarrow D \pi$  amplitude in the quark model:

$$A(D_i^* \rightarrow D_j \pi^a) = \frac{g_{\text{QM}}}{f_\pi} \sqrt{M_B^{\text{phys}} M_{D^*}^{\text{phys}}} (\lambda^a)_{ij} (\epsilon^* \cdot q). \quad (4.13)$$

<sup>12</sup>Strong decay widths are determined from (2.28) and (4.2), while radiative decay rates are calculated from (2.51) and (4.11).

For this to be in accordance with (4.1) predicted by chiral perturbation theory we are led to

$$g_{\text{QM}} \approx g \frac{Z_2}{Z_1} \frac{f_\pi}{f_0} \left[ \frac{M_D M_{D^*}}{M_B^{\text{phys}} M_{D^*}^{\text{phys}}} \right]^{1/2}. \quad (4.14)$$

Since  $Z_2 > Z_1$ ,  $f_\pi > f_0$ ,  $M_D > M_B^{\text{phys}}$ , and  $M_{D^*} > M_{D^*}^{\text{phys}}$ , it is evident that  $g < g_{\text{QM}}$ . By the same token, the relation between  $\beta$  and  $\beta_{\text{QM}}$  can be understood along the same line.

We next shift our attention to the heavy baryon sector. For the strong decay of heavy baryons, we shall only consider the decay  $\Sigma_c \rightarrow \Lambda_c \pi$  which is experimentally seen, although its rate has not been measured. (It is likely that no other  $B_6^* \rightarrow B_3 \pi$  or  $B_6^* \rightarrow B_6 \pi$  strong decays are kinematically allowed.) The decay rate for  $\Sigma_c \rightarrow \Lambda_c \pi$  is given by<sup>13</sup> [3]

$$\Gamma(\Sigma_c^{++} \rightarrow \Lambda_c^+ \pi^+) = \frac{1}{16\pi} \frac{(g_2)_{\text{eff}}^2 (M_{\Sigma_c} + M_{\Lambda_c})^2 [(M_{\Sigma_c} - M_{\Lambda_c})^2 - M_\pi^2]}{f_0^2 M_{\Sigma_c}} q, \quad (4.15)$$

where [see Eq. (3.25)]

$$(g_2)_{\text{eff}} = g_2 \frac{\sqrt{Z_2(\Sigma_c) Z_2(\Lambda_c)}}{Z_1'(\Sigma_c \rightarrow \Lambda_c \pi; 5(a))}, \quad (4.16)$$

which includes chiral-loop effects. Before examining the SU(3)-breaking effects induced by chiral loops in the electromagnetic decays of heavy baryons, it is instructive to examine the tree amplitudes of (3.29) to see what SU(3) violations are expected from the constituent quark model. From Eqs. (3.28) and (4.7), we find the quark model predictions

$$\begin{aligned} (a_2)_{\text{eff}}^{\text{QM}}(\Sigma_c^+ \rightarrow \Lambda_c^+ \gamma) &= a_2^{\text{QM}} \left[ \frac{2}{3} + \frac{1}{3} \frac{M_u}{M_d} \right] = 1.02 a_2^{\text{QM}} = 0.62e \text{ GeV}^{-1}, \\ (a_2)_{\text{eff}}^{\text{QM}}(\Xi_c'^+ \rightarrow \Xi_c^+ \gamma) &= a_2^{\text{QM}} \left[ \frac{2}{3} + \frac{1}{3} \frac{M_u}{M_s} \right] = 0.88 a_2^{\text{QM}} = 0.53e \text{ GeV}^{-1}, \\ (a_2)_{\text{eff}}^{\text{QM}}(\Xi_c'^0 \rightarrow \Xi_c^0 \gamma) &= \frac{1}{3} a_2^{\text{QM}} \left[ \frac{M_u}{M_s} - \frac{M_u}{M_d} \right] = -0.13 a_2^{\text{QM}} = -0.078e \text{ GeV}^{-1}, \end{aligned} \quad (4.17)$$

and

$$\begin{aligned} (a_1 - 8a_1')_{\text{eff}}^{\text{QM}}(\Sigma_c^{*0} \rightarrow \Sigma_c^0 \gamma) &= a_1^{\text{QM}} \frac{M_u}{M_d} - 8a_1' = 1.05 a_1^{\text{QM}} - 8a_1' = -1.45e \text{ GeV}^{-1}, \\ (a_1 - 8a_1')_{\text{eff}}^{\text{QM}}(\Omega_c^* \rightarrow \Omega_c \gamma) &= a_1^{\text{QM}} \frac{M_u}{M_s} - 8a_1' = 0.66 a_1^{\text{QM}} - 8a_1' = -1.07e \text{ GeV}^{-1}, \\ (a_1 - 8a_1')_{\text{eff}}^{\text{QM}}(\Xi_c'^*0 \rightarrow \Xi_c'^0 \gamma) &= \frac{1}{2} a_1^{\text{QM}} \left[ \frac{M_u}{M_d} + \frac{M_u}{M_s} \right] - 8a_1' = 0.86 a_1^{\text{QM}} - 8a_1' = -1.26e \text{ GeV}^{-1}, \\ (a_1 + 16a_1')_{\text{eff}}^{\text{QM}}(\Xi_c'^*+ \rightarrow \Xi_c'^+ \gamma) &= 3a_1^{\text{QM}} \left[ \frac{2}{3} - \frac{1}{3} \frac{M_u}{M_s} \right] + 16a_1' = 1.34 a_1^{\text{QM}} + 16a_1' = -0.49e \text{ GeV}^{-1}, \\ (a_1 + 16a_1')_{\text{eff}}^{\text{QM}}(\Sigma_c^{*+} \rightarrow \Sigma_c^+ \gamma) &= 3a_1^{\text{QM}} \left[ \frac{2}{3} - \frac{1}{3} \frac{M_u}{M_d} \right] + 16a_1' = 0.95 a_1^{\text{QM}} + 16a_1' = -0.104e \text{ GeV}^{-1}, \end{aligned} \quad (4.18)$$

where we have made use of the quark model predictions [10]

$$a_1^{\text{QM}} = -\frac{e}{3} \beta_{\text{QM}}, \quad a_2^{\text{QM}} = \frac{e}{2\sqrt{6}} \beta_{\text{QM}}, \quad (4.19)$$

with  $\beta_{\text{QM}} = 1/M_u$ . The parameter  $a_1'$  is predicted by heavy quark symmetry to be [10]

$$a_1' = \frac{e}{12m_c}. \quad (4.20)$$

From the lowest-order Lagrangian, we have the SU(3) re-

lations of (3.29). It is thus clear that a measurement of the decay rates of

- (i)  $\Sigma_c^{*0} \rightarrow \Sigma_c^0 \gamma$ ,  $\Xi_c'^*0 \rightarrow \Xi_c'^0 \gamma$ ,  $\Omega_c^* \rightarrow \Omega_c \gamma$ ,
- (ii)  $\Xi_c'^0 \rightarrow \Xi_c^0 \gamma$

relative to  $\Xi_c^+ \rightarrow \Xi_c^+ \gamma$  or  $\Sigma_c^+ \rightarrow \Lambda_c^+ \gamma$ ,

<sup>13</sup>Note that  $f_0$  is replaced by  $f_\pi$  in Ref. [3], since there we work in the tree approximation only.

$$(iii) \Xi_c'^{*\ast} \rightarrow \Xi_c^+ \gamma, \quad \Sigma_c'^{*\ast} \rightarrow \Sigma_c^+ \gamma$$

will provide a nice test of SU(3) breaking.

We are now ready to compare the quark model predictions with those from chiral perturbation theory using (3.24), (3.25) and (3.30) for heavy baryon's decays. There are six unknown parameters in the theory:  $\Lambda$ ,  $m_c$ ,  $g_1$ ,  $g_2$ ,  $a_1$ , and  $a_2$ . Unfortunately, there do not exist any experimental data for the heavy baryons to guide the choice of these parameters. It is clearly premature to make an all-out effort to study how the predictions vary with the parameters. To gain a general idea of how chiral perturbation theory is compared with the quark model, we minimize the number of parameters by setting  $\Lambda = 1$  GeV and  $m_c = 1.6$  GeV as before, and by making use of the quark model relations [10]

$$\begin{aligned} g_1 &= \frac{1}{3}g, \quad g_2 = -\left(\frac{2}{3}\right)^{1/2}g, \\ a_1 &= -\frac{e}{3}\beta, \quad a_2 = \frac{e}{2\sqrt{6}}\beta. \end{aligned} \quad (4.21)$$

The remaining two parameters  $g$  and  $\beta$  are finally fixed with the values favored by the available  $D^*$  decay data:

$$g = 0.52, \quad \beta = 0.26 \text{ GeV}^{-1}. \quad (4.22)$$

The relevant wave-function and vertex renormalization constants  $Z_2$ ,  $Z'_1$ , and  $Z''_1$  for various processes are given and

by (3.15), (3.22), (3.23), and (3.36)–(3.42). Numerically,

$$\begin{aligned} Z_2(\Lambda_c) &= 1.40, \quad Z_2(\Xi_c) = 1.83, \\ Z_2(\Sigma_c) &= 1.12, \quad Z_2(\Xi_c') = 1.14, \quad Z_2(\Omega_c) = 1.19 \end{aligned} \quad (4.23a)$$

and

$$Z'_1(\Sigma_c \rightarrow \Lambda_c \pi; 5(a)) = 1.07. \quad (4.23b)$$

From (4.15), (4.16), and (4.23) we find that

$$\Gamma(\Sigma_c'^{*\ast} \rightarrow \Lambda_c^+ \pi^+) = 1.89 \text{ MeV} \quad (4.24)$$

in the chiral Lagrangian approach as compared with 2.45 MeV in the quark model [3].

Vertex corrections to radiative decays are

$$\begin{aligned} Z_1(\Sigma_c'^{*\ast} \rightarrow \Sigma_c^+ \gamma) &= 0.77, \\ Z_1(\Sigma_c'^{*\ast} \rightarrow \Sigma_c^+ \gamma) &= 0.62, \\ Z_1(\Sigma_c'^{0*} \rightarrow \Sigma_c^0 \gamma) &= 0.92, \\ Z_1(\Xi_c'^{*\ast} \rightarrow \Xi_c^+ \gamma) &= 1.00, \\ Z_1(\Xi_c'^{0*} \rightarrow \Xi_c^0 \gamma) &= 0.78, \\ Z_1(\Omega_c^* \rightarrow \Omega_c \gamma) &= 0.63, \\ Z''_1(\Sigma_c'^{*\ast} \rightarrow \Lambda_c^+ \gamma) &= 0.88, \\ Z''_1(\Xi_c'^{*\ast} \rightarrow \Xi_c^+ \gamma) &= 0.87, \end{aligned} \quad (4.25)$$

and

$$\begin{aligned} \delta a_1(\Sigma_Q^{+1(*)} \rightarrow \Sigma_Q^+ \gamma; 6(c)) &= \delta a_1(\Xi_Q'^{-1/2(*)} \rightarrow \Xi_Q'^{-1/2} \gamma; 6(c)) = 0.24e \text{ GeV}^{-1}, \\ \delta a_1(\Omega_Q^{(*)} \rightarrow \Omega_Q \gamma; 6(c)) &= \delta a_1(\Sigma_Q^{0(*)} \rightarrow \Sigma_Q^0 \gamma; 6(c)) = 0.38e \text{ GeV}^{-1}, \\ \delta a_1(\Sigma_Q^{-1(*)} \rightarrow \Sigma_Q^- \gamma; 6(c)) &= \delta a_1(\Xi_Q'^{1/2(*)} \rightarrow \Xi_Q'^{1/2} \gamma; 6(c)) = 0.11e \text{ GeV}^{-1}, \\ \delta a_2(\Sigma_Q^{0(*)} \rightarrow \Lambda_Q \gamma; 7(c)) &= -0.08e \text{ GeV}^{-1}, \\ \delta a_2(\Xi_Q'^{1/2(*)} \rightarrow \Xi_Q'^{1/2} \gamma; 7(c)) &= -0.16e \text{ GeV}^{-1}, \\ \delta a_2(\Xi_Q'^{-1/2(*)} \rightarrow \Xi_Q'^{-1/2} \gamma; 7(a)+7(b)+7(c)) &= 0.15a_2 - 0.03e \text{ GeV}^{-1}. \end{aligned} \quad (4.26)$$

We get from Eqs. (3.30), (4.23a), and (4.25) and (4.26) that

$$\begin{aligned} (a_1 - 8a'_1)_{\text{eff}}(\Sigma_c'^{0*} \rightarrow \Sigma_c^0 \gamma) &= 1.08a_1 - 8a'_1 = -1.36e \text{ GeV}^{-1}, \\ (a_1 - 8a'_1)_{\text{eff}}(\Omega_c^* \rightarrow \Omega_c \gamma) &= 1.46a_1 - 8a'_1 = -1.68e \text{ GeV}^{-1}, \\ (a_1 - 8a'_1)_{\text{eff}}(\Xi_c'^{0*} \rightarrow \Xi_c^0 \gamma) &= 1.19a_1 - 8a'_1 = -1.45e \text{ GeV}^{-1}, \end{aligned} \quad (4.27a)$$

and

$$\begin{aligned} (a_1 + 16a'_1)_{\text{eff}}(\Xi_c'^{*\ast} \rightarrow \Xi_c^+ \gamma) &= 1.02a_1 + 16a'_1 = -0.05e \text{ GeV}^{-1}, \\ (a_1 + 16a'_1)_{\text{eff}}(\Sigma_c'^{*\ast} \rightarrow \Sigma_c^+ \gamma) &= 1.35a_1 + 16a'_1 = -0.35e \text{ GeV}^{-1}. \end{aligned} \quad (4.27b)$$

A comparison between (4.27) and (4.18) indicates that the two approaches give similar results for some processes such as  $\Sigma_c'^{0*} \rightarrow \Sigma_c^0 \gamma$  and  $\Xi_c'^{0*} \rightarrow \Xi_c^0 \gamma$ , while they give dramatically different results for others such as  $\Sigma_c'^{*\ast} \rightarrow \Sigma_c^+ \gamma$  and  $\Xi_c'^{*\ast} \rightarrow \Xi_c^+ \gamma$ . For the decay amplitude

$$A(B_6^* \rightarrow B_6 + \gamma) = \eta_2 \bar{u}(k_\mu \not{\epsilon} - \epsilon_\mu \not{k}) \gamma_5 u^\mu, \quad (4.28)$$

with  $\eta_2$  being given by Eq. (3.29), the corresponding decay width is [10]

$$\Gamma(B_6^* \rightarrow B_6 + \gamma) = \frac{k}{48\pi} \eta_2^2 \left[ 1 - \frac{m_f^2}{m_i^2} \right]^2 (3m_i^2 + m_f^2), \quad (4.29)$$

where  $m_i$  ( $m_f$ ) is the mass of the initial (final) baryon in the decay. This formula is presented here for completeness, and we will not give any predictions for the decay rates of spin- $\frac{3}{2}$  heavy baryons as their masses are still unknown.

As for the electromagnetic decays  $B_6 \rightarrow B_{\bar{3}} + \gamma$ , Eqs. (3.30), (3.29), and (4.23)–(4.26) lead to

$$\begin{aligned} (a_2)_{\text{eff}}(\Sigma_c^+ \rightarrow \Lambda_c^+ \gamma) &= 1.27a_2 = 0.67e \text{ GeV}^{-1}, \\ (a_2)_{\text{eff}}(\Xi_c'^+ \rightarrow \Xi_c^+ \gamma) &= 1.36a_2 = 0.72e \text{ GeV}^{-1}, \\ (a_2)_{\text{eff}}(\Xi_c'^0 \rightarrow \Xi_c^0 \gamma) &= 0.10a_2 = 0.05e \text{ GeV}^{-1}. \end{aligned} \quad (4.30)$$

Note that  $\Xi_c'^0 \rightarrow \Xi_c^0 \gamma$  receives two contributions, one from Fig. 7(a) and the other from Fig. 7(c), and there is a cancellation between the two. The sign of this amplitude in (4.30) is actually opposite to that in the quark model [cf. Eq. (4.17)]. With the formula [10]

$$\Gamma(B_6 \rightarrow B_{\bar{3}} + \gamma) = \frac{1}{\pi} \eta_1^2 k^3 \quad (4.31)$$

for the radiative decay amplitude

$$A(B_6 \rightarrow B_{\bar{3}} + \gamma) = \eta_1 \bar{u}_{\bar{3}} \sigma_{\mu\nu} k^\mu \epsilon^\nu u_6, \quad (4.32)$$

the decay rates of various decays are then predicted to be<sup>14</sup>

$$\begin{aligned} \Gamma(\Sigma_c^+ \rightarrow \Lambda_c^+ \gamma) &= 112 \text{ keV}, \\ \Gamma(\Xi_c'^+ \rightarrow \Xi_c^+ \gamma) &= 29 \text{ keV}, \\ \Gamma(\Xi_c'^0 \rightarrow \Xi_c^0 \gamma) &= 0.15 \text{ keV}, \end{aligned} \quad (4.33)$$

which should be compared with the corresponding quark model results: 93, 16, and 0.3 keV.

The predicted SU(3)-breaking patterns in chiral perturbation theory for radiative decays of charmed mesons and baryons are [see (4.12) and (4.27)]

$$\begin{aligned} \sum_{\text{pol}} |A(D_s^{*+} \rightarrow D_s^+ \gamma)|^2 &> \sum_{\text{pol}} |A(D^{*+} \rightarrow D^+ \gamma)|^2, \\ \sum_{\text{pol}} |A(\Omega_c^* \rightarrow \Omega_c \gamma)|^2 &> \sum_{\text{pol}} |A(\Sigma_c^{*0} \rightarrow \Sigma_c^0 \gamma)|^2 \\ &\sim \sum_{\text{pol}} |A(\Xi_c'^{*0} \rightarrow \Xi_c'^0 \gamma)|^2, \\ \sum_{\text{pol}} |A(\Sigma_c^{*+} \rightarrow \Sigma_c^+ \gamma)|^2 &\gg \sum_{\text{pol}} |A(\Xi_c'^{*+} \rightarrow \Xi_c'^+ \gamma)|^2, \end{aligned} \quad (4.34)$$

which are opposite to what expected from the quark

model [see (4.10), (4.17), and (4.18)]. It is thus extremely important to measure the decay rates of the above-mentioned modes to test the underlying mechanism of SU(3) violation.

We should reiterate the tentative nature of the discussion in this section. In the heavy meson case, the data for  $D^*$  are useful but not decisive in selecting the values of the parameters. Other important effects such as  $1/m_Q$  corrections have not been incorporated. The procedure employed here is by no means a best fit. The apparent agreement between the quark model and chiral perturbation theory is pleasing, but it should be taken with caution. In the heavy baryon sector, the situation is even more difficult. First of all, we do not have any experimental data. Second, there are many more parameters here than in the heavy meson sector. The choice of parameters based on (4.19)–(4.21) is necessarily *ad hoc*. The only virtue is that it provides a rule to fix the parameters. It will not be surprising if nature picks a very different choice from the present one. Third, the renormalization effects are very significant, as evident from (4.23) and (4.24). We may question the validity of chiral perturbation expansion.<sup>15</sup> Fourth, large cancellations occur sometimes. For all these reasons, the results obtained in this section should not be considered final. Rather, they make it clear that more experimental and theoretical works are needed.

## V. CONCLUSIONS

As we have emphasized before, the lowest-order low-energy dynamics of heavy mesons and heavy baryons is completely determined by the heavy quark symmetry and chiral symmetry, supplemented by the quark model. In order to gain a different perspective of our previous quark model calculations, we have investigated in the present paper chiral symmetry violation induced by the light current quark masses. Chiral corrections to the strong and electromagnetic decays of heavy hadrons are computed at the one-loop order. The leading chiral-loop effects are nonanalytic in the forms of  $m_q^{1/2}$  and  $m_q \ln m_q$ . We have also confirmed in chiral perturbation theory at the one-loop level the exact result in QCD that the heavy quark contributions to the  $M1$  transitions of heavy hadrons are not modified by light quark dynamics [see (2.47), (3.33b), and (3.35)]. Moreover, all consequences of heavy quark symmetry are not affected by chiral corrections. We then applied our results to the radiative and strong decays of charmed mesons and charmed baryons.

<sup>15</sup>The similar problem in the meson sector is less severe except for the  $D_s^{*+}$  decay. For  $g=0.52$ , we have  $Z_2(D^{*0})=Z_2(D^{*+})=1.18$ ,  $Z_2(D_s^{*+})=1.32$ , and all the  $Z_1$ 's are very close to unity for the strong decays, and  $Z_1(D^{*0} \rightarrow D^0 \gamma)=0.74$ ,  $Z_1(D^{*+} \rightarrow D^+ \gamma)=0.87$ ,  $Z_1(D_s^{*+} \rightarrow D_s^+ \gamma)=0.57$  for radiative decays.

<sup>14</sup>All the charmed baryon masses are taken from the Particle Data Group [21]. For the mass of  $\Xi_c'$ , we employ the hyperfine mass splitting  $m_{\Xi_c'} - m_{\Xi_c} \simeq 100 \text{ MeV}$  derived in Ref. [25].

We found in the meson sector that for a particular set of the parameters  $g$  and  $\beta$  inferred from the measured branching ratios of the  $D^{*0}$  and  $D^{*+}$  and the upper limit on the  $D^{*+}$  rate, the predictions of the strong and electromagnetic decays of the  $D^*$  mesons in the chiral Lagrangian approach are not very different from the quark model results except for the radiative decay of the  $D_s^{*+}$ . Using the quark model to relate the four unknown parameters in the baryon sector to  $g$  and  $\beta$ , we have computed the strong decay  $\Sigma_c \rightarrow \Lambda_c \pi$  and the radiative decays  $B_6^* \rightarrow B_6 + \gamma$  and  $B_6 \rightarrow B_{\bar{3}} + \gamma$ . We found that the chiral Lagrangian and quark model approaches in general give similar results for many processes, whereas they yield drastically different predictions for others such as  $\Sigma_c^{*+} \rightarrow \Sigma_c^+ \gamma$  and  $\Xi_c'^{*+} \rightarrow \Xi_c'^+ \gamma$ . Moreover, the predicted SU(3)-breaking patterns as shown in (4.34) are opposite to the quark model expectations. It is thus of great importance to measure the decay modes listed in (4.34) to test the underlying mechanism of SU(3) violation.

A more meaningful and improved comparison between theory and experiment has to wait until more data on heavy hadrons become available. In the meantime, it is important to have a better theoretical understanding of the corrections due to the  $1/m_Q$  effects. We believe that both SU(3) symmetry breaking and the  $1/m_Q$  effects should be considered simultaneously. We will return to this effort sometime in the future.

#### ACKNOWLEDGMENTS

One of us (H.Y.C.) wishes to thank Professor C. N. Yang and the Institute for Theoretical Physics at Stony Brook for their hospitality during his stay there for sabbatical leave. T.M.Y.'s work was supported in part by the National Science Foundation. This research was supported in part by the National Science Council of ROC under Contracts Nos. NSC83-0208-M001-012, NSC83-0208-M001-014, NSC83-0208-M001-015, and NSC83-0208-M008-009.

#### APPENDIX A

In this appendix we list some of the useful Feynman integrals which are relevant to this paper:

$$\int \frac{\Lambda^\epsilon d^n l}{(2\pi)^n} \frac{l_\mu}{(l^2 - m^2 + i\epsilon)(v \cdot l + i\epsilon)} = i v_\mu \frac{m^2}{16\pi^2} \ln \frac{\Lambda^2}{m^2}, \quad (\text{A1})$$

$$\int \frac{\Lambda^\epsilon d^n l}{(2\pi)^n} \frac{l_\mu l_\nu}{(l^2 - m^2 + i\epsilon)^2 (v \cdot l + i\epsilon)} = -i \frac{m}{16\pi} (g_{\mu\nu} - v_\mu v_\nu), \quad (\text{A2})$$

$$\int \frac{\Lambda^\epsilon d^n l}{(2\pi)^n} \frac{l_\mu l_\nu}{(l^2 - m^2 + i\epsilon)(v \cdot l + i\epsilon)^2} = -i (g_{\mu\nu} - 2v_\mu v_\nu) \frac{m^2}{16\pi^2} \ln \frac{\Lambda^2}{m^2}, \quad (\text{A3})$$

$$\begin{aligned} & \int \frac{\Lambda^\epsilon d^n l}{(2\pi)^n} \frac{l_\mu l_\nu}{(l^2 - m^2 + i\epsilon)[v \cdot (l + \tilde{k}) + \delta m + i\epsilon]} \\ &= -i \frac{m^3}{24\pi} (g_{\mu\nu} - v_\mu v_\nu) + i \frac{1}{16\pi^2} \ln \frac{\Lambda^2}{m^2} \{ (g_{\mu\nu} - 2v_\mu v_\nu)(v \cdot \tilde{k} + \delta m)m^2 - 2(g_{\mu\nu} - 4v_\mu v_\nu)(v \cdot \tilde{k})\delta m^2 \} \\ &+ i \frac{m}{16\pi} (g_{\mu\nu} - 3v_\mu v_\nu)(v \cdot \tilde{k})\delta m, \end{aligned} \quad (\text{A4})$$

$$\begin{aligned} & \int \frac{\Lambda^\epsilon d^n l}{(2\pi)^n} \frac{l_\mu l_\nu l_\alpha}{[(l+k)^2 - m^2 + i\epsilon](l^2 - m^2 + i\epsilon)(v \cdot l + i\epsilon)} \quad (\text{with } k^2=0 \text{ and } v \cdot k=0) \\ &= i \frac{m}{32\pi} \left\{ [(g_{\mu\nu} - v_\mu v_\nu)k_\alpha + \text{cyclic in } \mu, \nu, \alpha] + \frac{1}{2m^2} k_\mu k_\nu k_\alpha \right\} \\ &+ i \frac{m^2}{32\pi^2} \ln \frac{\Lambda^2}{m^2} \left\{ \left[ g_{\mu\nu} + \frac{2}{3m^2} k_\mu k_\nu \right] v_\alpha + \text{cyclic in } \mu, \nu, \alpha \right\} - 2v_\mu v_\nu v_\alpha, \end{aligned} \quad (\text{A5})$$

where the common factor

$$\frac{1}{\epsilon'} \equiv \frac{1}{\epsilon} - \frac{1}{2} \gamma_E + \frac{1}{2} \ln 4\pi, \quad (\text{A6})$$

with  $\epsilon = 4 - n$ , has been lumped into the logarithmic term  $\ln(\Lambda^2/m^2)$  as  $\Lambda$  is an arbitrary renormalization scale occurring in the dimensional regularization approach. Note that only the leading contributions linear in  $v \cdot \tilde{k}$  are retained in (A4). Our results for the integrals (A3) and (A4) are in agreement with Ref. [17]. Equation (A5) is

derived by assuming  $v \cdot k = 0$ , where  $k$  is the momentum of the outgoing photon which couples to heavy hadrons. This is a legitimate assumption as long as both incoming and outgoing hadrons are on shell. To evaluate above integrals, we first apply tensor decomposition as well as momentum expansions to reduce them into the prototypes

$$I_1(\alpha) = \int \frac{\Lambda^\epsilon d^n l}{(2\pi)^n} \frac{1}{(l^2 - m^2 + i\epsilon)^\alpha (v \cdot l + i\epsilon)} \quad (\text{A7})$$

and

$$I_2(\alpha) = \int \frac{\Lambda^\epsilon d^n l}{(2\pi)^n} \frac{1}{(l^2 - m^2 + i\epsilon)^\alpha (v \cdot l + i\epsilon)^2}. \quad (\text{A8})$$

We observe that all the external momenta have disappeared from the denominator due to the expansion

$$\frac{1}{(l+k)^2 - m^2} = \frac{1}{l^2 - m^2} \left[ 1 - \frac{2l \cdot k + k^2}{l^2 - m^2} \right] + \dots. \quad (\text{A9})$$

This expansion is a valid procedure since the momentum  $k$  is very soft in the current context. Similar types of expansions can be applied to Eq. (A4) for bringing up the residual momentum  $\tilde{k}$  to the numerator.

To carry out integrals  $I_1$  and  $I_2$ , the usual Feynman parametrization

$$\frac{1}{a^m b^n} = \frac{\Gamma(m+n)}{\Gamma(m)\Gamma(n)} \int_0^1 \frac{x^{m-1}(1-x)^{n-1} dx}{[ax + b(1-x)]^{m+n}} \quad (\text{A10})$$

does not allow one to shift the loop momentum  $l$  without destroying the structure of the integral. Hence it is convenient to combine denominators using the identity

$$\frac{1}{a^m b^n} = \frac{\Gamma(m+n)}{\Gamma(m)\Gamma(n)} \int_0^\infty \frac{2^n \lambda^{n-1} d\lambda}{(a + 2\lambda b)^{m+n}}, \quad (\text{A11})$$

which is obtained from (A10) by changing the variable  $x = 1/(1+2\lambda)$ . Sometimes the integration can even be done without combining denominators. We consider the integral  $I_1$  as an example to illustrate the importance of the  $i\epsilon$  terms presented in the denominator. We write

$$\begin{aligned} I_1(\alpha) &= \int \frac{\Lambda^\epsilon d^n l}{(2\pi)^n} \frac{1}{(l^2 - m^2 + i\epsilon)^\alpha (v \cdot l + i\epsilon)} \\ &= \frac{1}{2} \int \frac{\Lambda^\epsilon d^n l}{(2\pi)^n} \frac{1}{(l^2 - m^2 + i\epsilon)^\alpha} \\ &\quad \times \left[ \frac{1}{v \cdot l + i\epsilon} + \frac{1}{-v \cdot l + i\epsilon} \right]. \end{aligned} \quad (\text{A12})$$

The second line follows from the fact that  $I_1$  is invariant under the substitution  $l \rightarrow -l$ . Since

$$\frac{1}{v \cdot l + i\epsilon} = \mathcal{P} \frac{1}{v \cdot l} - i\pi \delta(v \cdot l), \quad (\text{A13})$$

the integral becomes

$$I_1(\alpha) = -i\pi \int \frac{\Lambda^\epsilon d^n l}{(2\pi)^n} \delta(v \cdot l) \frac{1}{(l^2 - m^2 + i\epsilon)^\alpha}. \quad (\text{A14})$$

Since  $I$  is a scalar integral, we can easily evaluate it by going to the rest frame of  $v$ . In the rest frame of  $v$ ,  $v^\mu = (1, \mathbf{0})$ , we find

$$I_1(\alpha) = -i\pi (-1)^\alpha \Lambda^\epsilon \int \frac{d^{n-1} l}{(2\pi)^n} \frac{1}{(l^2 + m^2 - i\epsilon)^\alpha}, \quad (\text{A15})$$

where  $l$  is a vector in  $(n-1)$ -dimensional space. Performing the angular integration gives

$$I_1(\alpha) = -\frac{i\pi (-1)^\alpha \Lambda^\epsilon}{(2\pi)^n} \frac{2\pi^{(n-1)/2}}{\Gamma((n-1)/2)} \int dl \frac{l^{n-2}}{(l^2 + m^2)^\alpha}. \quad (\text{A16})$$

Now the  $l$  integration is standard, which gives

$$\begin{aligned} I_1(\alpha) &= -\frac{i\pi (-1)^\alpha \Lambda^\epsilon}{(2\pi)^n} \\ &\quad \times \pi^{(n-1)/2} \frac{\Gamma(\alpha - (n-1)/2)}{\Gamma(\alpha)} (m^2)^{[(n-1)/2] - \alpha}. \end{aligned} \quad (\text{A17})$$

It is easy to see that  $I_1(\alpha)$  is finite for any integer  $\alpha$ . Taking  $n=4$  we have

$$I_1(\alpha) = -\frac{i(-1)^\alpha \sqrt{\pi}}{16\pi^2} \frac{\Gamma(\alpha - \frac{3}{2})}{\Gamma(\alpha)} (m^2)^{3/2 - \alpha}. \quad (\text{A18})$$

To evaluate  $I_2(\alpha)$ , it is more convenient to apply the identity (A11) since the principal part of the integral no longer cancels. By the power-counting argument, one expects  $I_2(1)$  to be logarithmically divergent. However, as we will show momentarily, such ultraviolet divergence will appear in the  $\lambda$  integration rather than in the momentum one. Therefore some care is needed in order to consistently treat the infinities. To illustrate this, let us first apply Eq. (A11) to combine denominators of  $I_2(1)$ . This procedure gives

$$I_2(1) = \int_0^\infty 8\lambda d\lambda \int \frac{\Lambda^\epsilon d^n l}{(2\pi)^n} \frac{1}{[l^2 - (m^2 + \lambda^2)]^3}. \quad (\text{A19})$$

It is obvious that no infinities arise in the momentum integration. Carrying out the momentum integration, we obtain

$$I_2(1) = -2i\pi^2 \Lambda^\epsilon \int_0^\infty d\kappa \frac{1}{\kappa + m^2}, \quad (\text{A20})$$

where we have changed the variable such that  $\kappa = \lambda^2$ . Apparently, the ultraviolet divergence now appears in the  $\kappa$  integration. To consistently implement the dimensional regularization, let us perform an analytic continuation on  $I_2(1)$  with the aid of

$$\int d^n l \frac{\partial}{\partial l_\mu} (l_\mu f(l)) = \int d^n l l_\mu \frac{\partial}{\partial l_\mu} f(l) + n \int d^n l f(l), \quad (\text{A21})$$

where  $f$  is an arbitrary function of  $l$ . The LHS of Eq. (A21) can be set to zero since the integrand is a total derivative. Now  $I_2(1)$  can be defined in terms of  $I_2(2)$  through Eq. (A21):

$$I_2(1) = -\frac{2m^2}{4-n} I_2(2). \quad (\text{A22})$$

Since  $I_2(2)$  is convergent, the infinity in  $I_2(1)$  manifests itself as a simple pole at  $n=4$ . To determine  $I_2(1)$  including its finite parts, one has to evaluate  $I_2(2)$  to  $O(4-n)$ . Applying Eq. (A11) gives

$$I_2(2) = \int_0^\infty 24\lambda d\lambda \int \frac{\Lambda^\epsilon d^n l}{(2\pi)^n} \frac{1}{[l^2 - (m^2 + \lambda^2)]^4}. \quad (\text{A23})$$

Carrying out both integrations we arrive at

$$I_2(2) = \frac{2i}{16\pi^2 m^2} \left[ 1 - \frac{\epsilon}{2}(\gamma_E - \ln\pi - 2\ln 2) + \frac{\epsilon}{2} \ln \frac{\Lambda^2}{m^2} \right]. \quad (\text{A24})$$

By Eq. (A21) we obtain

$$I_2(1) = -\frac{4i}{16\pi^2} \left[ \frac{1}{\epsilon} - \frac{1}{2}(\gamma_E - \ln\pi - 2\ln 2) + \frac{1}{2} \ln \frac{\Lambda^2}{m^2} \right]. \quad (\text{A25})$$

To compute any  $I_2(\alpha)$  with  $\alpha > 2$ , one may repeatedly apply Eq. (A14). The general result is given by

$$I_2(\alpha) = \frac{i}{16\pi^2 m^2} \frac{2(-m^2)^{2-\alpha}}{\alpha-1}, \quad (\text{A26})$$

with  $\alpha \geq 2$ .

Finally, the integral (A5) can also be carried out by combining the first two denominators via the conventional Feynman parametrization (A10), followed by another combination with the third denominator ( $v \cdot l + i\epsilon$ ) using the identity (A11). As a consequence,

$$\frac{1}{[(l+k)^2 - m^2 + i\epsilon](l^2 - m^2 + i\epsilon)(v \cdot l + i\epsilon)} = 4 \int_0^\infty d\lambda \int_0^1 dx \frac{1}{[(l+v\lambda+kx)^2 + x(1-x)k^2 - \lambda^2 - m^2]^3}. \quad (\text{A27})$$

After the momentum integration, the integration over  $x$  becomes trivial.

## APPENDIX B

In this appendix we explain the procedures used in Sec. III to obtain the results for strong and electromagnetic vertices, especially how the SU(3) group factors are defined and arrived at. We will consider two examples: one for a strong vertex and one for an electromagnetic vertex. For the strong vertex, we will take Fig. 4(b) with sextet baryons as the intermediate states. The corresponding tree amplitude can be written as

$$A(S_{ij}^\nu \rightarrow S_{kl}^\mu + \pi^a) = i \frac{3}{4} \frac{g_1}{f_0} \epsilon_{\mu\alpha\beta\nu} \bar{U}^\mu v^\alpha q^\beta \mathcal{U}^\nu \langle S_{kl} | \text{tr}(B^\dagger \lambda^a B) | S_{ij} \rangle, \quad (\text{B1})$$

where  $B$  is the sextet baryon matrix as defined in Eq. (3.2);  $|S_{ij}\rangle$  and  $|S_{kl}\rangle$  are, respectively, the SU(3) flavor wave functions for the initial and final baryons, such that

$$B_{mn} |S_{ij}\rangle = \frac{1}{\sqrt{2}} (\delta_{mi} \delta_{nj} + \delta_{mj} \delta_{ni}) |0\rangle \quad (i \neq j), \quad (\text{B2})$$

$$B_{mn} |S_{ii}\rangle = \delta_{mi} \delta_{ni} |0\rangle.$$

Hence, for the specific case of  $S_{ij} \rightarrow S_{ij} + \pi^3$ , we have

$$A(S_{ij}^\nu \rightarrow S_{ij}^\mu + \pi^3) = i \frac{3}{8} \frac{g_1}{f_0} \epsilon_{\mu\alpha\beta\nu} \bar{U}^\mu v^\alpha q^\beta \mathcal{U}^\nu (\lambda_{ii}^3 + \lambda_{jj}^3). \quad (\text{B3})$$

The loop contribution from Fig. 4(a) with sextet intermediate states can be written in the form

$$A_S(S_{ij}^\nu \rightarrow S_{kl}^\mu + \pi^a) = \sum_b \bar{U}^\mu M_{\mu\nu}(b) \mathcal{U}^\nu \langle S_{kl} | G(b) | S_{ij} \rangle, \quad (\text{B4})$$

where  $M_{\mu\nu}(b)$  is the contribution from the loop excluding the SU(3) matrices:

$$M_{\mu\nu}(b) = \left[ -i \frac{3g_1}{4f_0} \right]^3 \int \frac{d^4 l}{(2\pi)^4} \epsilon_{\mu\sigma\lambda\kappa} l^\lambda v^\kappa \epsilon_{\alpha\gamma\beta\delta} q^\beta v^\delta \epsilon_{\rho\nu\xi\zeta} (-l^\xi) v^\zeta \frac{i(-g^{\sigma\alpha} + v^\sigma v^\alpha)}{v \cdot l} \frac{i(-g^{\rho\gamma} + v^\rho v^\gamma)}{v \cdot l} \frac{i}{l^2 - m_{\pi^b}^2}, \quad (\text{B5})$$

where we have neglected the residual momentum  $\tilde{k}$  of the initial baryon and the external pion momentum  $q$  in the propagators since we are only interested in the leading-order contribution. Using the result (A3) for the integral we obtain

$$M_{\mu\nu}(b) = -2i \epsilon_{\mu\alpha\beta\nu} v^\alpha q^\beta \frac{1}{f_0} \left[ \frac{3}{4} g_1 \right]^3 \epsilon_{\pi^b}, \quad (\text{B6})$$

where  $\epsilon_{\pi^b}$  is defined in (2.22). The operator  $G(b)$  is a product of traces involving SU(3) matrices and the sextet baryon matrix  $B$ :

$$G(b) = \text{tr}(B^\dagger \lambda^b B) \text{tr}(B^\dagger \lambda^a B) \text{tr}(B^\dagger \lambda^b B). \quad (\text{B7})$$

Note that the adjacent intermediate  $B$ 's and  $B^\dagger$ 's in (B7) combine in pairs to form sextet "propagators" in the SU(3) flavor space: namely,

$$\langle B_{kl} B_{mn}^\dagger \rangle = \frac{1}{2} (\delta_{kn} \delta_{lm} + \delta_{km} \delta_{ln}). \quad (\text{B8})$$

Thus  $G(b)$  can be rewritten as

$$G(b) = \frac{1}{4} \text{tr} \{ B^\dagger \lambda^b \lambda^b B \lambda^a T + B^\dagger \lambda^b \lambda^a B \lambda^b T + B^\dagger \lambda^b B (\lambda^a \lambda^b)^T + B^\dagger \lambda^b \lambda^a \lambda^b B \}, \quad (\text{B9})$$

where the superscript  $T$  signifies the transposition of a matrix. Again, for the case of  $S_{ij} \rightarrow S_{ij} + \pi^3$ , the flavor matrix element can be easily worked out to be

$$\langle S_{ij} | G(b) | S_{ij} \rangle = \xi_{ij}, \quad (\text{B10})$$

where  $\xi_{ij}$  is given by (3.17). When (B3) and (B10) are combined we obtain

$$A_S(S_{ij}^v \rightarrow S_{ij}^u + \pi^3) = -2i \frac{1}{f_0} \epsilon_{\mu\alpha\beta\nu} \bar{U}^\mu v^\alpha q^\beta U^\nu \left[ \frac{3}{4} g_1 \right]^3 \sum_b \epsilon_{\pi^b} \xi_{ij}. \quad (\text{B11})$$

Adding up to the tree amplitude (B3), we find

$$A(S_{ij}^v \rightarrow S_{ij}^u + \pi^3) = i \frac{eg_1}{8f_0} \epsilon_{\mu\alpha\beta\nu} \bar{U}^\mu v^\alpha q^\beta U^\nu (\lambda_{ii}^3 + \lambda_{jj}^3) \times \left[ 1 - \frac{9}{4} g_1^2 \sum_b \frac{\epsilon_{\pi^b} \xi_{ij}}{\lambda_{ii}^3 + \lambda_{jj}^3} \right]. \quad (\text{B12})$$

The quantity in the square brackets of (B12) is the contribution to  $Z_1^{-1}$  due to the intermediate sextet baryons of Fig. 4(a). It agrees with the term proportional to  $g_1^2$  of Eq. (3.16).

The contribution to  $Z_1$  due to the antitriplet baryon intermediate states of Fig. 4(a) can be computed similarly. The SU(3) flavor ‘‘propagator’’ for an antitriplet is

$$\langle T_{kl} T_{mn}^\dagger \rangle = \delta_{kn} \delta_{lm} - \delta_{km} \delta_{ln}. \quad (\text{B13})$$

The difference in normalization between (B13) and (B8) is

$$M'_{\mu\nu}(b) = \left[ -i \frac{3g_1}{4f_0} \right]^2 (-ie) \int \frac{d^4 l}{(2\pi)^4} \epsilon_{\mu\beta\lambda\kappa} (l+k)^\lambda v^\kappa (-2l-k) \cdot \epsilon \epsilon_{\alpha\nu\gamma\delta} (-l)^\gamma v^\delta \frac{i}{(l+k)^2 - m_{\pi^b}^2} \frac{i}{l^2 - m_{\pi^b}^2} \frac{i(-g^{\alpha\beta} + v^\alpha v^\beta)}{v \cdot l}. \quad (\text{B17})$$

Note that the Goldstone bosons  $\pi^a$  and  $\pi^b$  on both sides of the electromagnetic vertex must have the same mass, which we denote as  $m_{\pi^b}$ . The integrals needed in (B17) are given in Appendix A. After neglecting a contribution to the convention current proportional to  $v \cdot \epsilon$ , we get the gauge-invariant result

$$M'_{\mu\nu}(b) = e \left[ \frac{3g_1}{4f_0} \right]^2 \frac{m_{\pi^b}}{16\pi} i (k_\mu \epsilon_\nu - k_\nu \epsilon_\mu). \quad (\text{B18})$$

The group factor operator  $G'(b)$  is given by

$$G'(b) = \sum_a \text{tr}(B^\dagger \lambda^b B) \text{tr}(B^\dagger \lambda^a B) \left\{ -\frac{1}{2} \text{tr}(\lambda^a [Q, \lambda^b]) \right\}. \quad (\text{B19})$$

Making use of the sextet propagator (B8) and the identity

$$\sum_a \lambda_{jk}^a \lambda_{mn}^a = 2(\delta_{jn} \delta_{km} - \frac{1}{3} \delta_{jk} \delta_{mn}), \quad (\text{B20})$$

we obtain

$$G'(b) = -\frac{1}{2} \text{tr} \{ B^\dagger \lambda^b [Q, \lambda^b] B + B^\dagger \lambda^b B [Q, \lambda^b]^T \}. \quad (\text{B21})$$

For the case  $S_{ij} \rightarrow S_{ij} + \gamma$ , we find

a result of how the matrices for a sextet and an antitriplet are defined [see (3.1) and (3.2)]. The minus sign in (B13) accounts for the antisymmetry of the antitriplet baryon matrix  $T$  (or  $B_{\bar{3}}$ ).

We now give an example of the calculation for a loop diagram in which a photon couples to Goldstone bosons. Consider the Feynman diagram of Fig. 6(c) with intermediate sextet baryons. The interactions of the Goldstone bosons with the electromagnetic vector potential  $A_\mu$  are introduced into Eq. (2.20) by the substitution

$$\partial_\mu \Sigma \rightarrow D_\mu \Sigma \equiv \partial_\mu \Sigma + ie A_\mu [Q, \Sigma]. \quad (\text{B14})$$

The electromagnetic vertex for  $\pi^a \rightarrow \pi^b + \gamma$  is given by

$$A(\pi^a \rightarrow \pi^b + \gamma) = -ie(2q - k) \cdot \epsilon \left\{ -\frac{1}{2} \text{tr}(\lambda^a [Q, \lambda^b]) \right\}, \quad (\text{B15})$$

where  $q$  and  $k$  are the momentum of  $\pi^a$  and the photon, respectively. The quantity in the square brackets is equal to 1 when the Goldstone boson has a unit positive charge. It will be part of the group factor defined below. Figure 6(c) with intermediate sextet baryons gives a contribution to  $S \rightarrow S + \gamma$ ,

$$A_S(S_{ij}^v \rightarrow S_{kl}^u + \gamma) = \sum_b \bar{U}^\mu M'_{\mu\nu}(b) U^\nu \langle S_{kl} | G'(b) | S_{ij} \rangle, \quad (\text{B16})$$

in a notation similar to (B4). We find

$$\langle S_{ij} | G'(b) | S_{ij} \rangle = -\frac{1}{4} \{ (\lambda^b [Q, \lambda^b])_{ii} + \lambda_{ii}^b [Q, \lambda^b]_{jj} (1 - \delta_{ij}) + \lambda_{ij}^b [Q, \lambda^b]_{ji} + (i \leftrightarrow j) \}. \quad (\text{B22})$$

As a consequence of the fact that  $Q$  is diagonal, we have

$$[Q, \lambda^b]_{jj} = 0, \quad (\text{B23a})$$

$$\lambda_{ij}^b [Q, \lambda^b]_{ji} + (i \leftrightarrow j) = 0. \quad (\text{B23b})$$

Finally,

$$\langle S_{ij} | G'(b) | S_{ij} \rangle = \bar{\xi}_{ij}, \quad (\text{B24})$$

where  $\bar{\xi}_{ij}$  is defined by (3.49). Combining (B18) and (B24) we obtain

$$A_S(S_{ij}^u \rightarrow S_{ij}^v + \gamma) = i \frac{3}{2} \bar{U}^\nu (Q_{ii} + Q_{jj}) (k_\nu \epsilon_\mu - k_\mu \epsilon_\nu) U^\mu \times \left[ \frac{e}{32\pi} \sum_b \frac{m_{\pi^b}}{f_0^2} \frac{3}{4} g_1^2 \bar{\xi}_{ij} \frac{1}{Q_{ii} + Q_{jj}} \right]. \quad (\text{B25})$$

The quantity in the square brackets gives rise to the term proportional to  $g_1^2$  in (3.48).

- [1] N. Isgur and M. B. Wise, *Phys. Lett. B* **232**, 113 (1989); **237**, 527 (1990).
- [2] M. B. Voloshin and M. A. Shifman, *Yad. Fiz.* **45**, 463 (1987) [*Sov. J. Nucl. Phys.* **45**, 292 (1987)].
- [3] T. M. Yan, H. Y. Cheng, C. Y. Cheung, G. I. Lin, Y. C. Lin, and H. L. Yu, *Phys. Rev. D* **46**, 1148 (1992); see also T. M. Yan, *Chin. J. Phys. (Taipei)* **30**, 509 (1992).
- [4] M. B. Wise, *Phys. Rev. D* **45**, R2188 (1992).
- [5] G. Burdman and J. Donoghue, *Phys. Lett. B* **280**, 287 (1992).
- [6] P. Cho, *Phys. Lett. B* **285**, 145 (1992).
- [7] P. Cho and H. Georgi, *Phys. Lett. B* **296**, 408 (1992); **300**, 410(E) (1993).
- [8] J. F. Amundson, C. G. Boyd, E. Jenkins, M. Luke, A. V. Manohar, J. L. Rosner, M. J. Savage, and M. B. Wise, *Phys. Lett. B* **296**, 415 (1992).
- [9] H. Y. Cheng, C. Y. Cheung, G. L. Lin, Y. C. Lin, T. M. Yan, and H. L. Yu, *Phys. Rev. D* **46**, 5060 (1992).
- [10] H. Y. Cheng, C. Y. Cheung, G. L. Lin, Y. C. Lin, T. M. Yan, and H. L. Yu, *Phys. Rev. D* **47**, 1030 (1993).
- [11] CLEO Collaboration, F. Butler *et al.*, *Phys. Rev. Lett.* **69**, 2041 (1992).
- [12] ACCMOR Collaboration, S. Barlrag *et al.*, *Phys. Lett. B* **278**, 480 (1992).
- [13] H. Y. Cheng, C. Y. Cheung, G. L. Lin, Y. C. Lin, T. M. Yan, and H. L. Yu, *Phys. Rev. D* **49**, 2490 (1994).
- [14] A. Manohar and H. Georgi, *Nucl. Phys.* **B234**, 189 (1984).
- [15] S. Weinberg, *Physica* **96A**, 327 (1979).
- [16] J. Gasser and H. Leutwyler, *Nucl. Phys.* **B250**, 465 (1985).
- [17] P. Cho, *Nucl. Phys.* **B396**, 183 (1993).
- [18] B. Grinstein, E. Jenkins, A. Manohar, M. Savage, and M. B. Wise, *Nucl. Phys.* **B380**, 369 (1992).
- [19] R. Fleischer, *Phys. Lett. B* **303**, 147 (1993).
- [20] J. L. Goity, *Phys. Rev. D* **46**, 3929 (1992).
- [21] Particle Data Group, K. Hikasa *et al.*, *Phys. Rev. D* **45**, S1 (1992).
- [22] C. A. Dominguez and E. de Rafael, *Ann. Phys. (N.Y.)* **174**, 372 (1987); J. Gasser and H. Leutwyler, *Phys. Rep.* **87**, 77 (1982).
- [23] CLEO Collaboration, D. Bortoletto *et al.*, *Phys. Lett.* **69**, 2046 (1992).
- [24] L. Randall and E. Sather, *Phys. Lett. B* **303**, 345 (1993); J. L. Rosner and M. B. Wise, *Phys. Rev. D* **47**, 343 (1993); J. L. Goity, *Phys. Lett. B* **303**, 337 (1993); E. Jenkins, Report No. CERN-TH.6765/92, 1992 (unpublished).
- [25] M. J. Savage and M. Wise, *Nucl. Phys.* **B326**, 15 (1989).